Molecular mechanisms that enhance synapse stability despite persistent disruption of the spectrin/ankyrin/microtubule cytoskeleton

Catherine M. Massaro, Jan Pielage, and Graeme W. Davis

Department of Biochemistry and Biophysics, Program in Neuroscience, University of California, San Francisco, San Francisco, CA 94158

Loss of spectrin or ankyrin in the presynaptic motoneuron disrupts the synaptic microtubule cytoskeleton and leads to disassembly of the neuromuscular junction (NMJ). Here, we demonstrate that NMJ disassembly after loss of α-spectrin can be suppressed by expression of a Wld^S transgene, providing evidence for a Wallerian-type degenerative mechanism. We then identify a second signaling system. Enhanced MAPK-JNK-Fos signaling suppresses NMJ disassembly despite loss of presynaptic α-spectrin or ankyrin2-L. This signaling system is activated after an acute cytoskeletal disruption, suggesting an endogenous role during neurological stress. This signaling system also includes delayed, negative feedback via the JNK phosphatase *puckered*, which inhibits JNK-Fos to allow NMJ disassembly in the presence of persistent cytoskeletal stress. Finally, the MAPK-JNK pathway is not required for baseline NMJ stabilization during normal NMJ growth. We present a model in which signaling via JNK-Fos functions as a stress response system that is transiently activated after cytoskeletal disruption to enhance NMJ stability, and is then shut off allowing NMJ disassembly during persistent cytoskeletal disruption.

Introduction

We have previously screened for mutations in genes that are critical for synaptic stability at the *Drosophila* neuromuscular junction (NMJ; Eaton et al., 2002; Eaton and Davis, 2005; Pielage et al., 2005, 2008). When mutated, these genes cause the presynaptic motoneuron terminal to retract from the muscle fiber in a distal-to-proximal manner, leaving behind an unopposed postsynaptic apparatus that no longer receives motoneuron input (Eaton et al., 2002; Eaton and Davis, 2005; Pielage et al., 2005, 2008; Koch et al., 2008). These genes include α- and β-*spectrin* (Pielage et al., 2005), *ankyrin2* (Koch et al., 2008; Pielage et al., 2008), as well as genes coding for components of the dynein–dynactin complex (Eaton et al., 2002). It is currently unknown whether these mutations represent a cellular stress that triggers an active process of synapse disassembly and retraction at the NMJ, or whether these mutations disrupt cellular mechanisms that directly stabilize the NMJ and therefore cause a passive structural collapse of the presynaptic terminal. Spectrin and ankyrin2 are prominent cellular components that establish and maintain cell shape (Bennett and Davis, 1983; Bennett and Lambert, 1991; Bennett and Gilligan, 1993). If it is possible to suppress synapse retraction in these mutant animals, then one might be able to distinguish between the mechanisms responsible for structural integrity of the NMJ, and the mechanisms involved in the retraction or elimination of the NMJ.

Here, we demonstrate that synapse retraction after loss of α-spectrin can be significantly delayed by overexpression of the *wallerian degeneration slow* (Wld^S) transgene (Zhai et al., 2008; Avery et al., 2009; Conforti et al., 2009), as well as by enhanced bone morphogenetic protein (BMP) trophic signaling. Thus, our new data demonstrate that the disassembly of the *Drosophila* NMJ can be suppressed after a severe cytoskeletal perturbation, and that this process may have mechanistic similarities with Wallerian-type degeneration.

We then use this system to define a novel stabilizing signaling system at the *Drosophila* NMJ. The focus of this signaling system is the immediate early gene (IEG) *fos*. There is evidence to support both a neuroprotective and neurodegenerative role

Correspondence to Graeme W. Davis: gdavis@biochem.ucsf.edu

J. Pielage's present address is Friedrich Miescher Institute, 4058 Basel, Switzerland.

Abbreviations used in this paper: ALS, amyotrophic lateral sclerosis; BMP, bone morphogenetic protein; MT, microtubule; NMJ, neuromuscular junction.

Supplemental material can be found at:
http://doi.org/10.1083/jcb.200903166

The Rockefeller University Press $30.00
J. Cell Biol. Vol. 187 No. 1 101–117
www.jcb.org/cgi/doi/10.1083/jcb.200903166

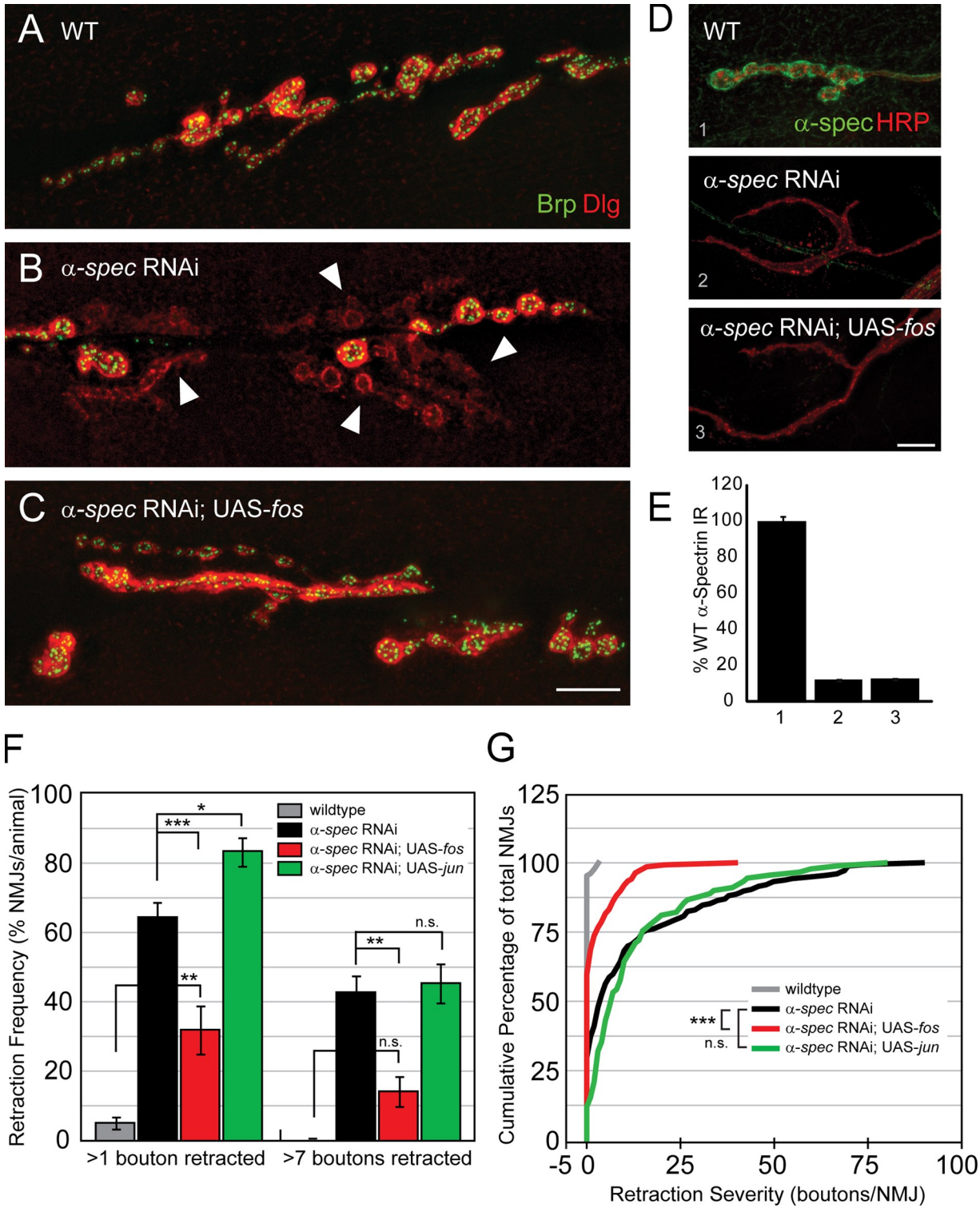

Figure 1. **Overexpression of Fos, but not Jun, suppresses synaptic instability at the NMJ.** (A–C) Representative images of muscle 6/7 NMJs stained for the presynaptic active zone protein Brp (green) and postsynaptic Dlg (red). (A) A wild-type NMJ shows Brp in apposition to Dlg throughout the NMJ. (B) An NMJ lacking presynaptic α-spectrin shows a large retraction (arrowheads), encompassing over 50% of the NMJ. (C) A similar loss of presynaptic innervation is not seen when Fos is expressed presynaptically, even in the absence of presynaptic α-spectrin. (D) Image of a wild-type animal (top) with α-spectrin expression (green) visible both in the muscle and innervating axon (as visualized by HRP). Expression of UAS–α-*spectrin*–dsRNA both neuronally and in the muscle eliminates α-spectrin staining throughout the NMJ (middle). Elimination of α-spectrin is not altered by concomitant expression of UAS-*fos* (bottom). (E) α-Spectrin immunoreactivity is quantified at 12 NMJs per genotype. (F and G) Quantification of retraction frequency (F) is measured as the average percentage of NMJs with >1 or >7 boutons retracted. Retraction severity (G) is measured as the number of boutons per NMJ that are retracted and the data are plotted as a cumulative frequency histogram for each genotype. Wild type = w^{1118} (n = 128 NMJs/30 animals). α-*spec* RNAi = $elav^{C155}$-GAL4/+; 2x UAS–α-*spectrin*–dsRNA (n = 177 NMJs/18 animals). α-*spec* RNAi; UAS-*fos* = elavC155-GAL4/+; 2x UAS–α-*spectrin*–dsRNA; UAS-*fos* (n = 137 NMJs/14 animals). α-*spec* RNAi; UAS-*jun* = $elav^{C155}$- GAL4/+; 2x UAS–α-*spectrin*–dsRNA; UAS-*jun* (n = 90 NMJs/9 animals). Error bars represent SEM;

for Fos. Fos expression is up-regulated in vivo in response to acute brain injury (e.g., ischemia or seizure induction) (Dragunow et al., 1994; Walton et al., 1998, 1999a; Cho et al., 2001). However, it is unclear whether Fos is mediating the resulting neuronal apoptosis or functioning in a neuroprotective pathway. A neurodegenerative function is supported by the observation that genetic elimination of c-Fos can be protective in light-induced retinal degeneration (Hafezi et al., 1997). In contrast, a number a studies have correlated c-Fos and/or upstream signaling molecules with neuroprotection (Walton et al., 1999b; Mabuchi et al., 2001; Lonze et al., 2002; Mantamadiotis et al., 2002; Palop et al., 2003; Saura et al., 2004). Here, we demonstrate that overexpression of Fos effectively reverses many of the hallmark phenotypes of synapse disassembly that are observed in animals lacking presynaptic α-spectrin. However, our data suggest that the stabilizing activity provided by endogenous Fos is only transient. Increased Fos protein induces the activity of a negative feedback signaling system that may, ultimately, allow synapse retraction and elimination to proceed in the presence of a persistent cellular stress.

Results

Assaying retraction of the presynaptic motoneuron terminal at the *Drosophila* NMJ

We previously published an assay for synapse integrity at the *Drosophila* NMJ (Eaton et al., 2002; Eaton and Davis, 2005; Pielage et al., 2005, 2008; Koch et al., 2008) that is similar to assays of synapse stability used at the vertebrate NMJ (Pun et al., 2006). In this assay we use neural-specific antibodies to label the presynaptic motoneuron terminal and simultaneously label the postsynaptic muscle membrane folds (Eaton et al., 2002; Eaton and Davis, 2005; Pielage et al., 2005, 2008). In wild-type animals, there is a precise alignment of pre- and postsynaptic markers throughout the *Drosophila* larval NMJ. However, mutations that disrupt synaptic integrity result in sites where the presynaptic nerve terminal retracts, leaving behind well-organized postsynaptic muscle membrane folds with clusters of postsynaptic glutamate receptors.

Fos overexpression suppresses presynaptic retraction after depletion of presynaptic α-spectrin

The NMJ in a wild-type animal rarely shows evidence of synapse retraction, and when retractions are observed they almost never encompass more than two boutons (Fig. 1 A). In contrast, neuronal expression of UAS–*α-spectrin* RNAi results in frequent and severe synapse retractions. In some cases these retractions can completely eliminate the presynaptic nerve terminal both anatomically and electrophysiologically (Fig. 1; see also Pielage et al., 2005). Here, we demonstrate that animals coexpressing UAS–*α-spectrin* RNAi and UAS-*fos* have significantly fewer and less severe synapse retractions at the NMJ compared with animals expressing UAS–*α-spectrin* RNAi alone (Fig. 1, C, F, and G). This result suggests that increased Fos signaling can suppress synapse destabilization caused by loss of presynaptic α-spectrin. To further investigate this possibility, several controls were performed. First, we controlled for the possibility that coexpression of UAS-*fos* diluted the amount of available GAL4, thereby decreasing the efficiency of UAS–*α-spectrin* RNAi. We controlled for this possibility by coexpressing an inert transgene, UAS-*mRFP(myr)*, along with UAS–*α-spectrin* RNAi. In these animals we see no suppression of synapse retraction frequency or severity (retraction frequency compared with UAS–*α-spectrin* RNAi alone, $P = 0.2$, $n = 79$; retraction severity compared with UAS–*α-spectrin* RNAi alone, $P = 0.25$, $n = 79$). Thus, dilution of GAL4 cannot account for the UAS-*fos*–dependent suppression of synapse retraction. As an additional control, we directly assayed presynaptic α-spectrin protein levels. Because muscle expression of α-spectrin masks our ability to observe presynaptic α-spectrin within the NMJ, we first assayed α-spectrin protein levels in the presynaptic axon just before innervation of the muscle. We find that α-spectrin protein is still absent from the presynaptic axon when UAS-*fos* is coexpressed with UAS–*α-spectrin* RNAi (Fig. S1). Identical results were obtained analyzing the axons of second-instar animals, demonstrating that α-spectrin knockdown occurs early in larval development despite coexpression of UAS-*fos* with UAS–*α-spectrin* RNAi (unpublished data). In addition, we show that simultaneous pre- and postsynaptic expression of UAS–*α-spectrin* RNAi severely depletes *α-spectrin* from the NMJ and coexpression of UAS-*fos* is without effect (Fig. 1, D and E). Thus, the efficiency and extent of α-spectrin knockdown by RNAi is not altered by the expression of UAS-*fos*. Finally, examination of synapse morphology in animals overexpressing UAS-*fos* in a wild-type background confirms previous observations that UAS-*fos* expression alone is not sufficient to drive synaptic growth or otherwise alter synapse morphology (unpublished data and Sanyal et al., 2002). Thus, improved synapse integrity is not a secondary consequence of accelerated synaptic growth. Together, these data suggest that expression of UAS-*fos* enhances synapse stability in the absence of presynaptic α-spectrin.

We next confirmed that presynaptic expression of UAS–*α-spectrin* RNAi causes a significant electrophysiological deficit at the NMJ (Fig. 2). In these experiments UAS–*α-spectrin* RNAi is coexpressed with UAS-*mRFP(myr)* as a control (see Fig. 2 legend). Then we asked whether coexpression of UAS-*fos* with UAS–*α-spectrin* RNAi would improve synaptic transmission as well as synapse stability. We find that UAS-*fos* coexpression significantly improves every measure of synaptic function when compared with animals that express UAS–*α-spectrin* RNAi. In animals coexpressing UAS-*fos* and UAS–*α-spectrin* RNAi presynaptically the average EPSP amplitude is significantly rescued

P values for retraction frequency were determined using one-way ANOVA with post-hoc Tukey-Kramer; P values for retraction severity were determined using a Kruskal-Wallis test with a post-hoc Dunn's test for multiple comparisons: *, $P < 0.05$; **, $P < 0.01$; ***, $P < 0.001$. Statistical differences remain when comparisons are made using Student's *t* test. Bar = 10 µm.

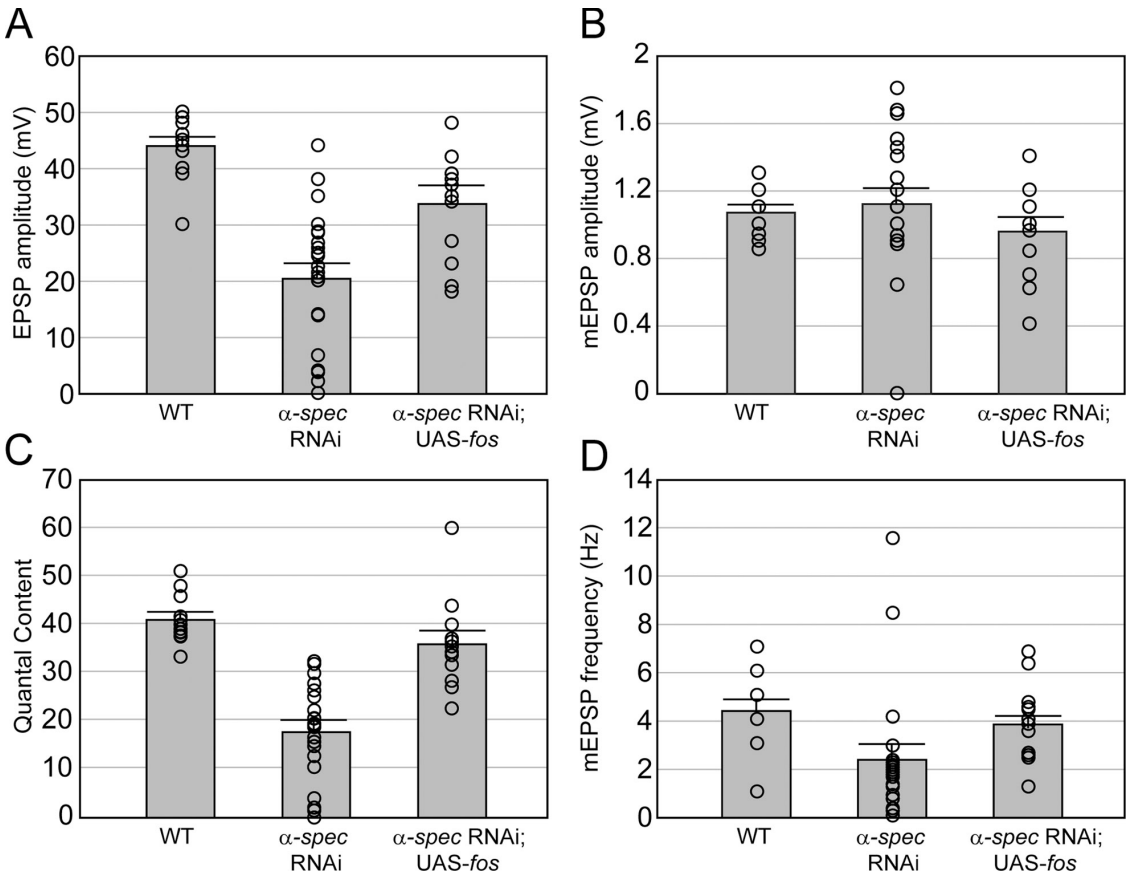

Figure 2. **Overexpression of Fos rescues synaptic function after loss of presynaptic α-spectrin.** (A–D) Average EPSP amplitude (A), mEPSP amplitude (B), quantal content (C), and mEPSP frequency (D) are plotted for three genotypes. Averages are shown in bar graph format. Superimposed on each bar are the individual averages for each parameter recorded from a single NMJ. There is a significant decrease in EPSP amplitude ($P < 0.001$) and quantal content ($P < 0.001$) in α-*spec* RNAi animals compared with wild type. There is a significant increase in average EPSP amplitude and quantal content toward wild-type levels by coexpression of UAS-*fos* (EPSP amplitude comparing α-*spec* RNAi to α-*spec* RNAi; UAS-*fos*: $P < 0.01$) (quantal content comparing α-*spec* RNAi to α-*spec* RNAi; UAS-*fos*, $P < 0.001$). Wild type = w^{1118} ($n = 13$ NMJs). α-*spec* RNAi = *elav*^{C155}-GAL4/+; 2x UAS–α-*spectrin*–dsRNA; UAS-*mRFP*(myr) ($n = 21$ NMJs). α-*spec* RNAi; UAS-*fos* = *elav*^{C155}-GAL4/+; 2x UAS–α-*spectrin*–dsRNA; UAS-*fos* ($n = 12$). P values were determined using one-way ANOVA with post-hoc Tukey-Kramer. Statistical differences remain when comparisons are made using Student's *t* test.

toward wild-type values (Fig. 2 A), and the average quantal content and mini frequency are not statistically different from wild type (Fig. 2, C and D). This demonstrates that UAS-*fos* coexpression improves synaptic function to near wild-type levels despite the severe depletion of presynaptic α-spectrin protein. Collectively, these data suggest that synapse retraction after depletion of the spectrin skeleton is not simply due to collapse of neuronal architecture, but reflects a process of synapse destabilization that can be significantly suppressed by overexpression of Fos.

Finally, as a control, we asked whether UAS-*fos* expression could suppress synapse retraction in the *ank2-L* mutant background (Pielage et al., 2008). NMJ retraction in *ank2-L* mutants is significantly more severe than that observed after RNAi-dependent depletion of presynaptic spectrin (Fig. S2). Although the number of NMJs that show evidence of retraction is unchanged in *ank2-L* animals that also overexpress presynaptic Fos, the severity of NMJ retraction is significantly decreased (Fig. S2). In addition, we find a significant reduction in the number of NMJs that are completely eliminated when UAS-*fos* is expressed presynaptically in the *ank2-L* mutant (Fig. S2). Finally, NMJ morphology more closely resembles wild type when UAS-*fos* is expressed in the *ank2-L* mutant (Fig. S2). In conclusion, ectopic expression of Fos confers synapse-stabilizing activity that slows the process of NMJ retraction despite the presence of a persistent cellular stress in *ank2-L* mutants.

Fos overexpression suppresses NMJ retraction despite a persistent disruption of the presynaptic MT cytoskeleton

Disruption of the presynaptic microtubule (MT) cytoskeleton is a common feature observed during synapse retraction at the *Drosophila* NMJ (Eaton and Davis, 2005; Pielage et al., 2005) and in many other forms of neuronal retraction and degeneration (Zhai et al., 2003; Luo and O'Leary, 2005; Hoopfer et al., 2006). Indeed, it has been proposed that disruption of neuronal microtubules could be causative for Wallerian-type neuronal degeneration (Zhai et al., 2003). It has been shown previously that presynaptic knockdown of α-spectrin causes a severe disruption of the Futsch-stabilized microtubule cytoskeleton at the *Drosophila* NMJ (Pielage et al., 2005). This result is repeated here (Fig. 3, A and B). In wild-type animals, the Futsch-positive MTs extend as a narrow filament throughout the NMJ (Fig. 3 A). After presynaptic

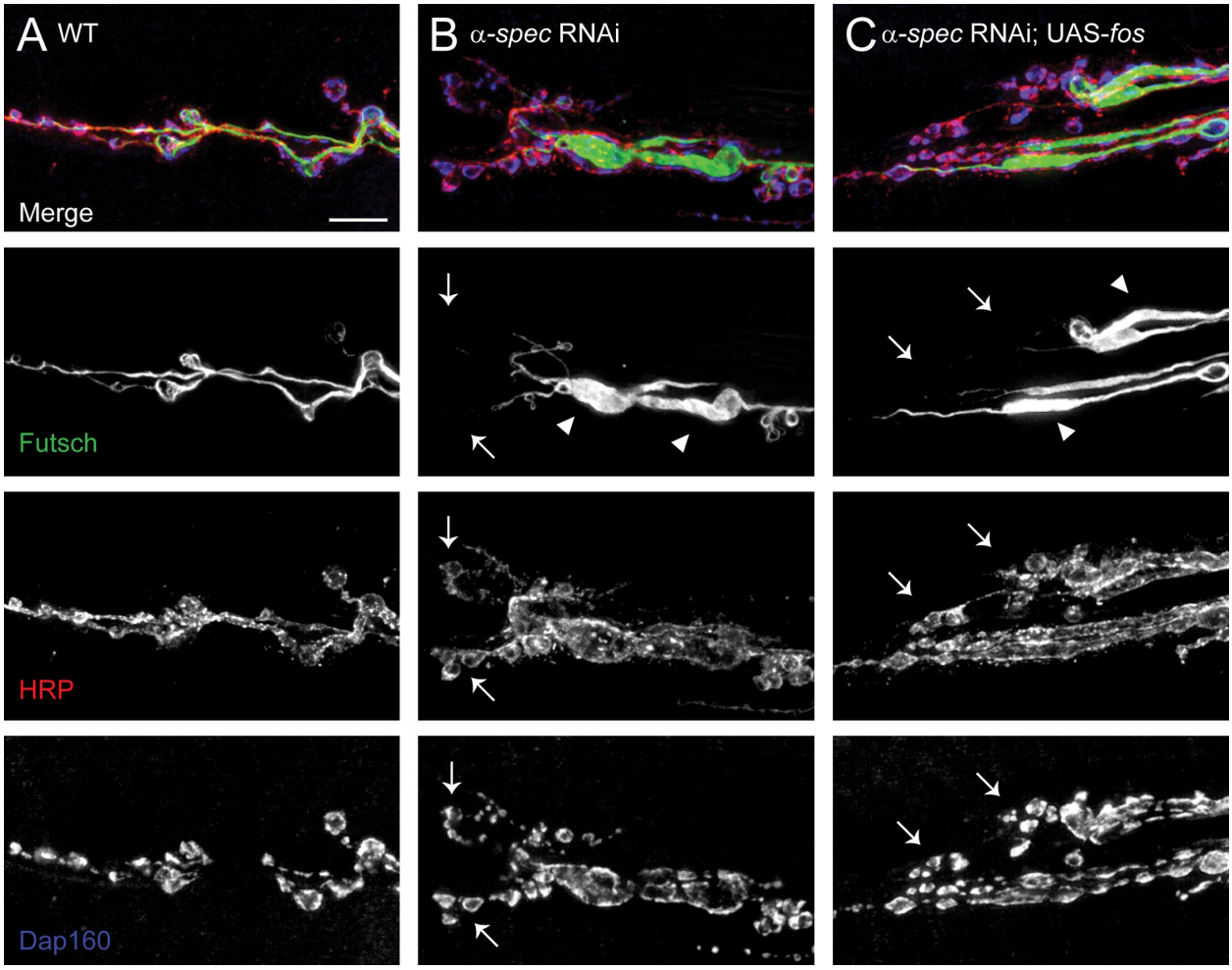

Figure 3. **Overexpression of Fos suppresses instability despite persistent microtubule disruption.** (A–C) Representative images of muscle 6/7 NMJs stained for the microtubule-associated protein Futsch (green; second row), the presynaptic membrane marker HRP (red; third row), and the presynaptic protein Dap160 (blue; bottom row). (A) A wild-type NMJ. (B) An NMJ lacking presynaptic α-spectrin shows disorganized Futsch staining. Accumulation of Futsch within boutons (arrowheads) and a lack of Futsch staining in distal boutons (arrows) can be observed. (C) Neuronal overexpression of Fos does not restore microtubule integrity. Distal boutons lacking Futsch staining (arrows), as well as large accumulations of Futsch (arrowheads) are still observed. Wild type = w^{1118}. α-*spec* RNAi = $elav^{C155}$-GAL4/+; 2x UAS–α-*spectrin*–dsRNA. α-*spec* RNAi; UAS-*fos* = $elav^{C155}$-GAL4/+; 2x UAS–α-*spectrin*–dsRNA; UAS-*fos*. Bar = 10 µm.

α-spectrin knockdown, the Futsch staining becomes disorganized and accumulates in large presynaptic swellings (Fig. 3 B).

One possible mechanism by which UAS-*fos* expression could stabilize the NMJ is through the production of molecules that re-stabilize the MT cytoskeleton at the NMJ. However, we find that the Futsch-positive MTs remain disorganized when UAS-*fos* is expressed in animals lacking presynaptic α-spectrin (Fig. 3 C). Importantly, this MT phenotype is unaltered even though the frequency and severity of NMJ retraction is significantly decreased. These observations indicate that Fos does not achieve synapse stability by restoring the stability or organization of the presynaptic MT cytoskeleton. Ultimately, we cannot rule out a partial, qualitative improvement in MT organization caused by UAS-*fos* overexpression. However, because UAS-*fos* expression does not restore α-spectrin protein to the NMJ and because α-spectrin is linked to MT organization via Ank2-L (Pielage et al., 2008), we consider this unlikely.

Previously, loss of presynaptic spectrin and ankyrin2-L has been correlated with altered organization of the synaptic cell adhesion molecules Fasciclin II (FasII) and Neuroglian (Nrg, the L1 homologue in *Drosophila*) (Pielage et al., 2005, 2008). Fasciclin II is a homophilic cell adhesion molecule necessary for synapse stability at this NMJ (Schuster et al., 1996). Therefore, we asked whether UAS-*fos*–dependent suppression of synaptic retraction might be mediated through up-regulation of one or both of these cell adhesion molecules. However, we find no evidence for a Fos-dependent increase in either FasII or Nrg protein at the NMJ (Fig. S3) that could explain enhanced NMJ stability.

Overexpression of Wld^S delays synapse retraction

It remains unclear whether the retraction of the presynaptic nerve terminal at the *Drosophila* NMJ is molecularly related to a developmental pruning process, akin to synapse elimination at the developing vertebrate NMJ, or whether it is related to neurodegeneration. Several lines of evidence have been used to argue that retraction of the motoneuron terminal at the *Drosophila*

NMJ is a degenerative event. First, elimination of previously functional NMJs is not a spontaneous event that occurs during normal development (Keshishian et al., 1996; Pielage et al., 2005, 2008). Second, mutations in genes that cause NMJ retraction in *Drosophila* have similarly been shown to play a role in neural degeneration in vertebrate model systems and humans (Parkinson et al., 2001; LaMonte et al., 2002; Hafezparast et al., 2003; Puls et al., 2003; Ligon et al., 2005; Ikeda et al., 2006; Levy et al., 2006; Bennett and Healy, 2008). Finally, the retraction of the motoneuron terminal is not preceded by motoneuron cell death (Eaton et al., 2002), and we have again confirmed this finding using a tunnel assay, examining wild-type and mutant CNS (unpublished data).

Recently, a molecular distinction has been made between the mechanisms responsible for developmental pruning of neuronal arbors and neurodegeneration. Wld^S is a spontaneously occurring dominant genetic aberration that fuses the 5′ end of *ube4b* and the *nmnat* gene (Lyon et al., 1993; Ring and Martinez Arias, 1993; Martín-Blanco et al., 1998; Mack et al., 2001). In vertebrates, the Wld^S mutation has been shown to slow Wallerian degeneration as well as other forms of neural degeneration (Perry et al., 1990, 1991; Wang et al., 2001, 2002; Ferri et al., 2003; Sajadi et al., 2004; Fischer et al., 2005; Luo and O'Leary, 2005; Hoopfer et al., 2006). In *Drosophila*, neuronal expression of a Wld^S transgene is sufficient to suppress neurodegeneration caused by axon transection (Hoopfer et al., 2006). However, in both *Drosophila* and vertebrate systems, Wld^S does not alter the process of developmental pruning of neuronal arborizations (Parson et al., 1997; Hoopfer et al., 2006). Therefore, we asked whether expression of the Wld^S transgene could suppress or slow the process of presynaptic retraction at the *Drosophila* NMJ.

Here, we demonstrate that animals neuronally coexpressing UAS–*α-spectrin* RNAi and UAS-Wld^S have significantly fewer and less severe synapse retractions compared with animals expressing UAS–*α-spectrin* RNAi alone (Fig. 4, B–E). Expression of UAS-Wld^S in a wild-type background has no effect on synaptic stability (unpublished data). These data are consistent with the conclusion that loss of α-spectrin induces a degenerative retraction of the presynaptic nerve terminal.

In vertebrate systems, the withdrawal of trophic factors from cultured motoneurons also induces a neurodegenerative response, and elevated expression of trophic signaling molecules can suppress neuromuscular degeneration in mouse models of amyotrophic lateral sclerosis (ALS) (Pun et al., 2006). At the *Drosophila* NMJ, BMP signaling functions as a trophic signaling system that supports NMJ growth (Aberle et al., 2002), and it has been shown that impaired BMP signaling causes synapse retraction at the NMJ (Eaton et al., 2002). Therefore, we asked whether neuronal expression of the BMP ligand *glass bottom boat* (*gbb*) could suppress synapse retraction after depletion of α-spectrin. Here, we show that neuronal coexpression of UAS-*gbb* with UAS–*α-spectrin* RNAi significantly suppresses the frequency and severity of NMJ retractions compared with expression of UAS–*α-spectrin* RNAi alone (Fig. 4, F and G; see also Materials and methods section for supplemental discussion relevant to this figure). Collectively, these data support the conclusion that retraction of the presynaptic motoneuron terminal at the *Drosophila* NMJ after loss of α-spectrin may be related to neurodegenerative processes in vertebrate systems.

Evidence for the induction of Fos-MAP kinase signaling after cytoskeletal disruption

Because the overexpression of UAS-*fos* is sufficient to suppress neuromuscular retraction, we sought to determine whether Fos protein levels are altered after expression of UAS–*α-spectrin* RNAi. Available Fos antibodies do not work well in situ, but can reliably report a 50% decrease in Fos protein in heterozygous *fos*/+ null mutant animals on Western blots (Fig. 5 B, top row) (the *fos* gene is also called *kayak* [*kay*] in *Drosophila* and the terms are used interchangeably). When we assayed Fos protein levels from the CNS of third-instar larvae that express UAS–*α-spectrin* RNAi throughout development and have significant NMJ retraction, we find no change in total Fos protein compared with controls (Fig. 5 B, bottom row). Thus, neuromuscular retraction is not correlated with a persistent change in Fos protein relative to controls.

Because Fos is an immediate early gene, we next considered the possibility that Fos protein levels transiently increase at some time during larval development after the loss of α-spectrin and the ensuing cytoskeletal disruption. To test this hypothesis, we acutely disrupted the neuronal cytoskeleton, in vivo, and assayed Fos protein levels. Pharmacological reagents to disrupt spectrin are not available. However, loss of α-spectrin results in a severe disruption of the underlying microtubule cytoskeleton (Fig. 3; Pielage et al., 2005). We reasoned that pharmacological perturbation of MTs might represent a similar, generalized, cytoskeletal stress, though clearly not identical to that caused by the developmental loss of α-spectrin. Several prior studies support such a conclusion (Zhai et al., 2003; Luo and O'Leary, 2005; Hoopfer et al., 2006). Therefore, we assayed Fos protein levels after disruption of the neuronal microtubules through application of 50–100 µM nocodazole (Noc) to larval neuromuscular preparations. This concentration of Noc efficiently disrupts the dynamic population of microtubules in *Drosophila* motoneuron axons and at the *Drosophila* NMJ without an immediate effect on Futsch-stabilized microtubule organization (unpublished data). We assayed Fos protein in animals incubated in Noc for either 30 min or 2 h (Fig. 5, E and F). At the 30-min time point, we observe a highly significant, greater than twofold increase in Fos protein levels compared with controls. At the 2-h time point, Fos levels have returned to baseline. These data are consistent with a rapid induction and decay of Fos protein after perturbation of the neuronal microtubule cytoskeleton. Because Fos overexpression is sufficient to suppress neuromuscular degeneration, we suggest that the increase in endogenous Fos protein may provide a transient stabilizing effect after cytoskeletal disruption.

Fos is embedded within a negative feedback signaling system that includes the dual-specificity, VH1 family phosphatase *puckered* (*puc*) (Fig. 5 A). Increased Fos activity leads to elevation of *puckered* transcription, decreased JNK activity and, ultimately, decreased Fos phosphorylation (Fig. 5 A) (Ring and Martinez Arias, 1993; Martín-Blanco et al., 1998; Agnès et al., 1999; Dobens et al., 2001). We asked whether this negative

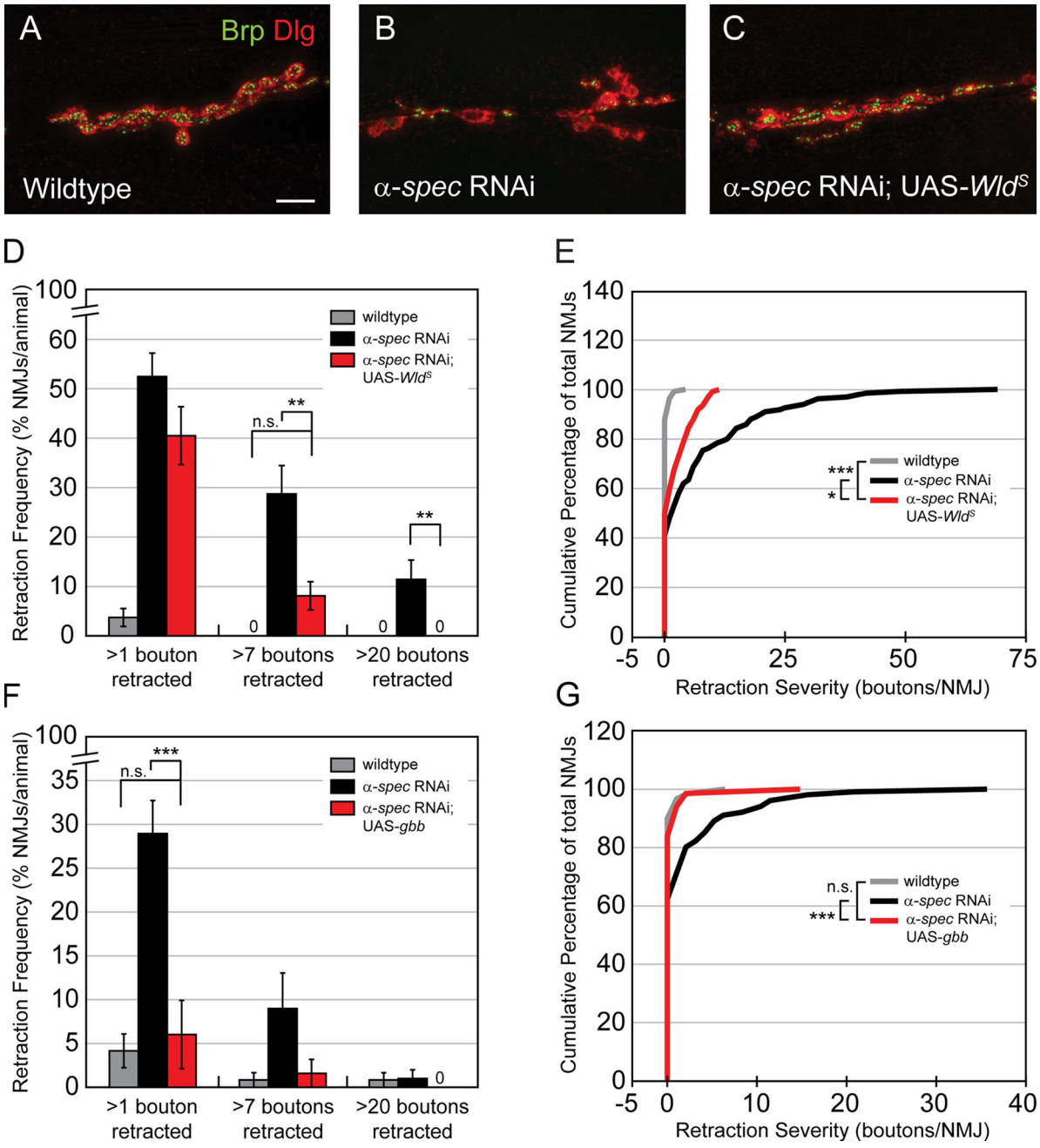

Figure 4. **Wld^S expression and potentiation of trophic signaling suppress instability at the NMJ in animals lacking presynaptic α-spectrin.** (A–C) Representative images of muscle 6/7 NMJs stained for the presynaptic active zone protein Brp (green) and postsynaptic Dlg (red). (A) A wild-type NMJ. (B) An NMJ lacking presynaptic α-spectrin shows a large retraction, encompassing a majority of the NMJ. (C) Neuronal expression of UAS-Wld^S slows the synaptic retraction process. (D and E) Wld^S decreases the severity of synaptic instability as well as the frequency of larger retraction events. Retraction frequency (D) is measured as the average percentage of NMJs with >1 or >7 boutons retracted. Retraction severity (E) is measured as the number of boutons per NMJ that are retracted and the data are plotted as a cumulative frequency histogram for each genotype. Wild type = w^{1118} (n = 137 NMJs/14 animals). α-*spec* RNAi = *elav*^{C155}-GAL4/+; 2x UAS–α-*spectrin*–dsRNA (n = 134 NMJs/14 animals). α-*spec* RNAi; UAS-*Wld*^{S} = *elav*^{C155}-GAL4/+; 2x UAS–α-*spectrin*–dsRNA; UAS-*Wld*^{S} (n = 127 NMJs/13 animals). (F and G) Neuronal expression of UAS-*gbb* decreases the severity (F) and frequency (G) of synaptic retractions. Wild type = w^{1118} (n = 119 NMJs/12 animals). α-*spec* RNAi = *elav*^{C155}-GAL4/+; UAS–α-*spectrin*–dsRNA (n = 100 NMJs/10 animals). α-*spec* RNAi; UAS-*gbb* = *elav*^{C155}-GAL4/+; UAS–α-*spectrin*–dsRNA; UAS-*gbb* (n = 67 NMJs/7 animals). Error bars represent SEM; P values for retraction frequency were determined using one-way ANOVA with post-hoc Tukey-Kramer; P values for retraction severity were determined using a Kruskal-Wallis test with a post-hoc Dunn's test for multiple comparisons: *, P < 0.05; **, P < 0.01; ***, P < 0.001. Statistical differences remain when comparisons are made using Student's *t* test. Bar = 10 µm.

feedback system might be induced after cytoskeletal disruption. To do so, we monitored the activity of a previously published *puckered* reporter (Martín-Blanco et al., 1998; Dobens et al., 2001). First, we validated the use of this reporter by showing that there is a statistically significant ~50% reduction in reporter activity in the heterozygous null *fos*/+ mutant background that parallels the observed 50% reduction in Fos protein (Fig. 5 C). We then find that there is a highly significant (greater than

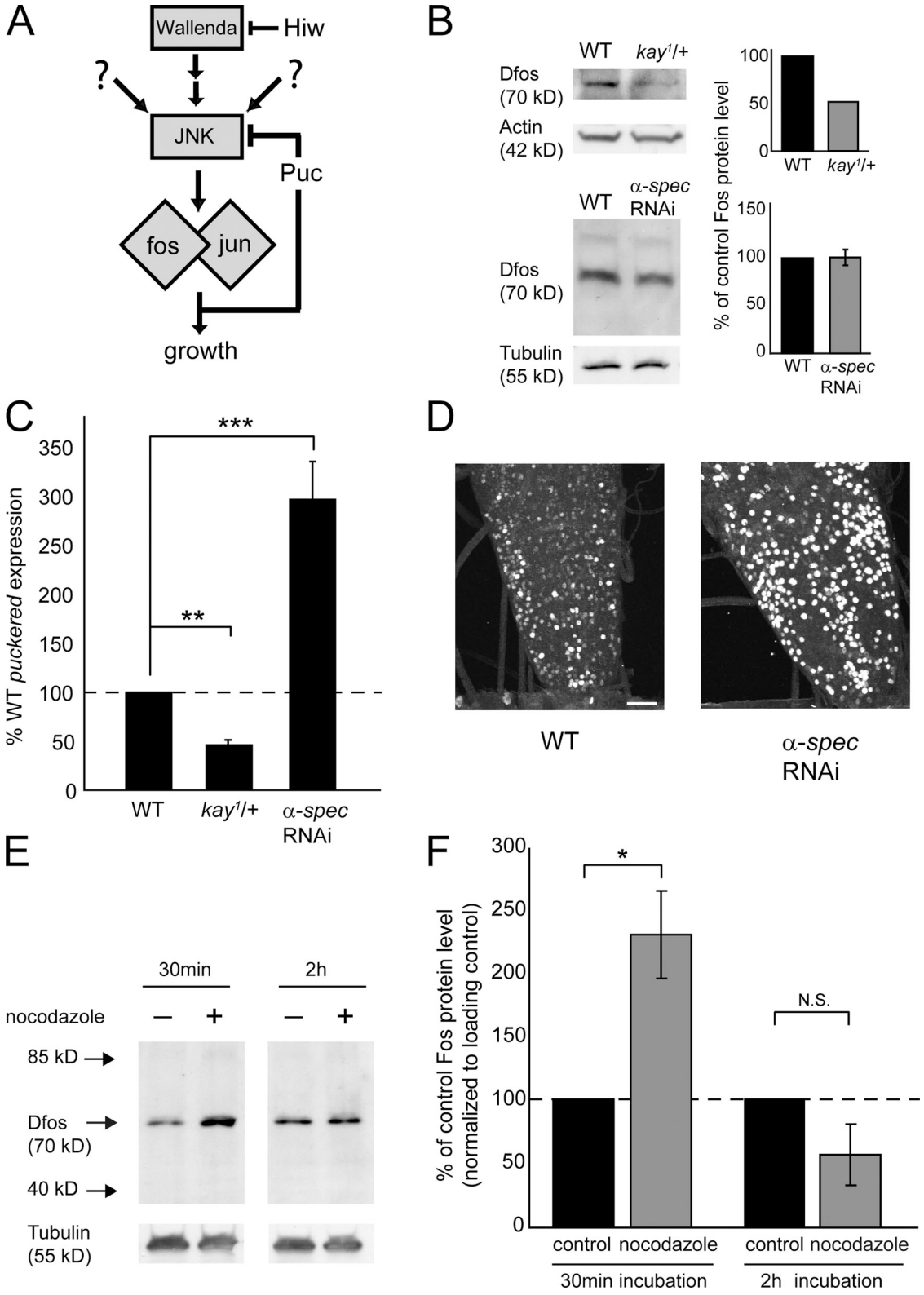

Figure 5. **Fos-MAP kinase signaling is induced after cytoskeletal disruption.** (A) Schematic diagram representing MAPK signaling that converges on Fos. Puckered (Puc) is shown as both a downstream target of Fos and Jun, as well as an upstream regulator of Fos and Jun activity through negative regulation of the upstream MAPK, Jun-Kinase (JNK). (B) Representative Western blot lanes and corresponding quantification for different genotypes. Images show bands for Dfos and the corresponding loading control for those lanes (tubulin or actin). Quantification shows average Fos protein levels normalized to loading control levels. Fos band intensity for each lane was normalized to the loading control band intensity for the same lane. Fos protein is decreased by 50% in kay^1/+ animals, confirming the specificity of the antibodies (data are aggregated from two different experiments with different anti-Fos antibodies). Wild type (top) = w^{1118} (6 CNS total). kay^1/+ (6 CNS total). Wild type (bottom) = w^{1118} (12 CNS total). α-*spec* RNAi = $elav^{C155}$-GAL4/+; 2x UAS–α-*spectrin*–dsRNA (12 CNS total). (C and D) puckered reporter is induced in the CNS in animals lacking presynaptic α-spectrin. (C) β-Gal levels are quantified in

twofold) induction of *puckered* reporter expression in the *α-spectrin* RNAi animals (Fig. 5 C). A similar induction of the *puckered* reporter can also be observed in central neurons, confirming the neuronal expression of this signaling pathway as well as a neuronal induction of this pathway in response to loss of α-spectrin (Fig. 5 D). One interpretation is that an initial elevation of Fos protein induced a persistent elevation in *puckered* transcription. Persistent activity of this negative feedback would constitutively inhibit Fos activity and prevent reactivation of elevated Fos protein during a persistent cytoskeletal perturbation. If the induction of Puckered-dependent negative feedback signaling favors NMJ retraction in the presence of a cytoskeletal perturbation, then loss-of-function mutations in the *puckered* gene might function similar to UAS-*fos* overexpression and suppress NMJ disassembly in animals lacking α-spectrin. Therefore, we went on to test this hypothesis genetically.

Mutations in the JNK phosphatase *puckered* suppress synapse retraction after loss of presynaptic α-spectrin

Homozygous *puckered* mutations are embryonic lethal. Therefore, we asked whether a hypomorphic loss-of-function *puckered* allelic combination could suppress synapse retraction in the background of animals expressing UAS–*α-spectrin* RNAi in neurons. First, we find that the *puckered* hypomorphic mutation alone did not show any significant defects in synapse stability compared with wild type (Fig. 6, A, B, E, and F). We then assayed synapse stability in the *elav*-GAL4; UAS–*α-spectrin* RNAi/+; puc^{1}/puc^{A251} double-mutant animals. We find that the presence of the *puckered* mutation significantly improves synapse stability as shown by a statistically significant decrease in both retraction frequency and severity (Fig. 6, C–F). Note that it was necessary, due to genetic considerations, to initiate synapse retractions by expressing a single copy of the UAS–*α-spectrin* RNAi transgene. A single copy of the RNAi transgene results in a less severe (though still highly significant) synapse retraction phenotype (see Materials and methods for supplemental discussion). These data support a model in which transient Fos activity is initially stabilizing, but is then attenuated by the induction of negative feedback via *puckered*. To further test this model, we examined mutations in a second gene, *highwire*, which has been previously shown to negatively regulate MAPK protein levels and Fos (Collins et al., 2006).

Mutations in *highwire* suppress synapse retraction after loss of presynaptic α-spectrin

The *highwire* gene encodes a large protein with putative E3 ubiquitin ligase activity (Wan et al., 2000; Aberle et al., 2002; Wu et al., 2005). In both *Drosophila* and *Caenorhabditis elegans*, the *highwire* (or *RPM-1*) mutation leads to increased levels of the MAP3K protein encoded by *wallenda* (*Drosophila*) or *dlk* (*C. elegans*) (Nakata et al., 2005; Collins et al., 2006). In *Drosophila*, the *highwire* mutation leads to increased synaptic growth that is dependent upon *wallenda*, *JNK*, and *fos* (Collins et al., 2006). Therefore, we tested whether *highwire*-dependent activation of Fos could suppress synapse retraction after loss of presynaptic α-spectrin. In these experiments, two copies of the UAS–*α-spectrin* RNAi transgene were used (as shown in Fig. 1).

First, we find that the presence of a heterozygous *highwire/+* mutation in the background of animals that express UAS–*α-spectrin* RNAi neuronally causes a slight but statistically significant suppression of synapse retraction severity (Fig. 7 F). There is also a trend toward a lower frequency of synapse retractions, though this is not statistically significant (Fig. 7 E). Importantly, in these animals, the NMJ is not overgrown, demonstrating that improved synapse stability can occur without a change in bouton number. Next, we analyzed synapse stability in animals harboring a hemizygous *highwire* mutation (*highwire/Y*) that also neuronally express UAS–*α-spectrin* RNAi. A hemizygous *highwire* mutation does not have any effect on stability in a wild-type background (Fig. 7, C, E, and F). However, we observe that a hemizygous *highwire* mutation results in a strong, statistically significant suppression of both synapse retraction frequency and severity in animals lacking presynaptic α-spectrin (Fig. 7, D–F). It is possible that NMJ overgrowth contributes to the suppression of synapse retraction in this experiment. However, because *highwire/+* can partially suppress synapse retractions without causing NMJ overgrowth, we speculate that NMJ overgrowth is not required to achieve increased synapse stability after loss of presynaptic α-spectrin. This is further supported by the demonstration that Fos overexpression suppresses synapse retraction without inducing NMJ overgrowth. Together these data support our model in which induction of negative feedback signaling via *puckered* attenuates the stabilizing activity of Fos, leading to more rapid NMJ disassembly. It should also be noted that the stabilizing activity of the *hiw* mutation could be due to elevated BMP signaling in this background (McCabe et al., 2004), which we have shown to be sufficient to suppress NMJ retraction (Fig. 4).

Evidence that Map kinase signaling is not required for NMJ stability

Finally, we asked whether the MAPK-Fos signaling pathway is required to prevent synapse retraction at the NMJ during normal development. First, we overexpressed the *puckered*

wild-type animals, $kay^{1}/+$ animals, and animals lacking presynaptic α-spectrin. Wild type = $puc^{A251.1F3}/+$ (6 animals). $kay^{1}/+$ = $kay^{1}/puc^{A251.1F3}$ (3 animals). α-*spec* RNAi = $elav^{C155}$-GAL4/+; $puc^{A251.1F3}/+$; 2x UAS–α-*spectrin*–dsRNA (6 animals). (D) Representative images of ventral nerve cords stained with an antibody against β-Gal to visualize expression of the puckered reporter in the CNS of a wild-type animal and an animal lacking presynaptic α-spectrin. (E and F) Representative Western blot lanes (E) and corresponding quantification (F) for control and nocodazole-treated animals. Images show bands for Dfos and the corresponding loading control for those lanes (tubulin). Quantification shows average Fos protein levels normalized to loading control levels. Fos band intensity for each lane was normalized to the loading control band intensity for the same lane. Quantification shows a greater than twofold increase in Fos protein after 30 min of nocodazole incubation. All animals = w^{1118} (30 min: control $n = 3$ trials/15 CNS total, nocodazole $n = 3$ trials/15 CNS total; 2 h control $n = 4$ trials/20 CNS total, nocodazole $n = 5$ trials/25 CNS total). Error bars represent SEM; P values were determined using Student's *t* test: *, P < 0.05; **, P < 0.01; ***, P < 0.001. Bar = 20 µm.

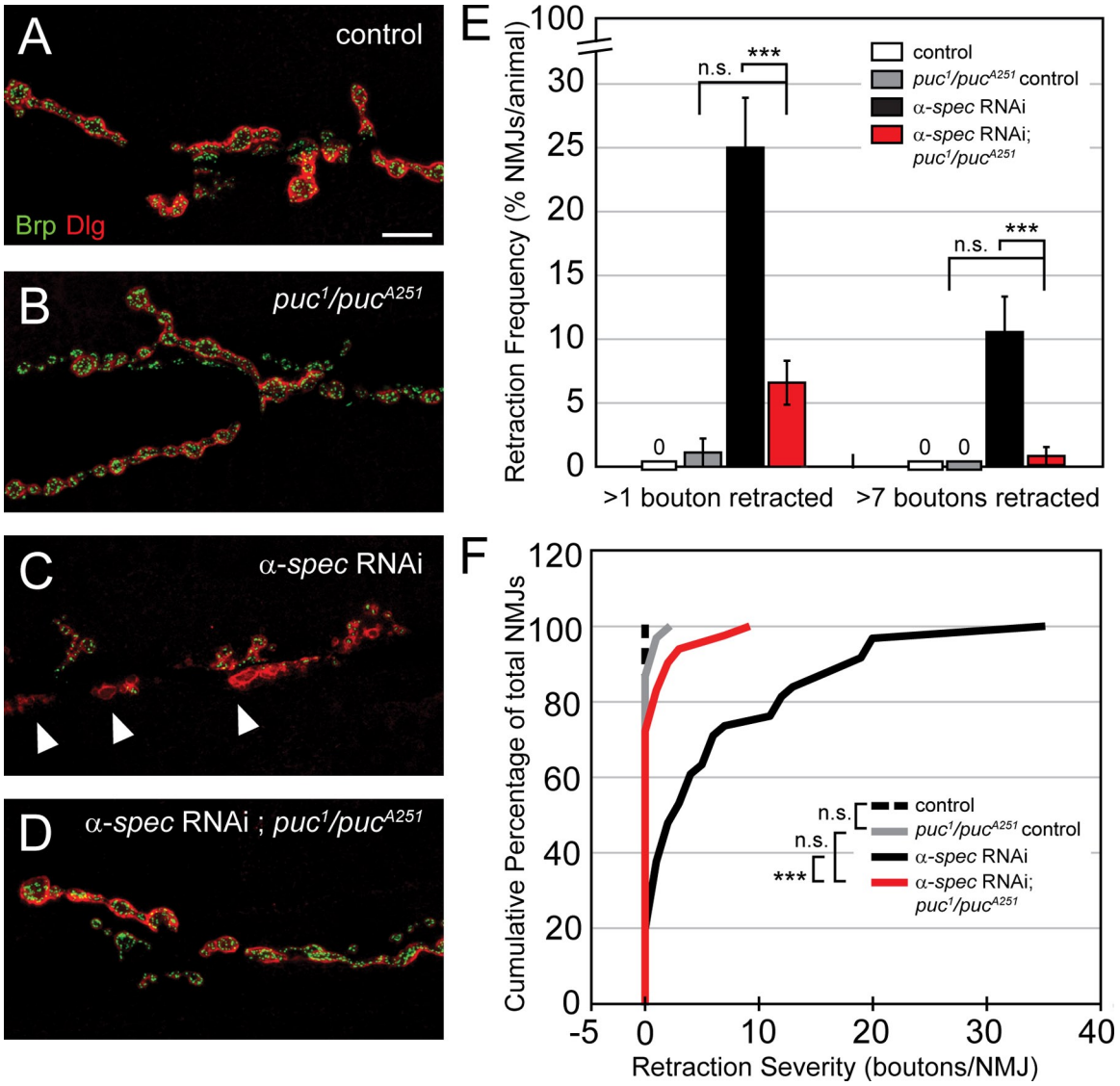

Figure 6. **Loss of Puckered suppresses synaptic instability at the NMJ.** (A–D) Representative images of muscle 6/7 NMJs stained for the presynaptic active zone protein Brp (green) and postsynaptic Dlg (red). (A) A control NMJ. (B) An NMJ from a larva with mutations in puckered ($puc^{1}/puc^{A251.1F3}$) shows maintenance of this apposition of pre and postsynaptic markers. (C) An NMJ lacking presynaptic α-spectrin shows a severe retraction (arrowheads). (D) This phenotype is suppressed in puckered mutants. (E and F) Quantification of retraction frequency (E) is measured as the average percentage of NMJs with >1 or >7 boutons retracted. Retraction severity (F) is measured as the number of boutons retracted per NMJ and the data are plotted as a cumulative frequency histogram for each genotype. control = 1x UAS–α-*spectrin*–dsRNA (no GAL4) (n = 39 NMJs/4 animals). puc^{1}/puc^{A251} control = 1x UAS–α-*spectrin*–dsRNA; $puc^{1}/puc^{A251.1F3}$ (no GAL4) (n = 97 NMJs/10 animals). α-*spec* RNAi = $elav^{C155}$-GAL4/+ or $elav^{C155}$-GAL4/Y; 1x UAS-α-*spectrin*–dsRNA (n = 96 NMJs/10 animals). α-*spec* RNAi; puc^{1}/puc^{A251} = $elav^{C155}$-GAL4/+; 1x UAS–α-*spectrin*–dsRNA; $puc^{1}/puc^{A251.1F3}$ (n = 136 NMJs/14 animals). Error bars represent SEM; P values for retraction frequency were determined using one-way ANOVA with post-hoc Tukey-Kramer; P values for retraction severity were determined using a Kruskal-Wallis test with a post-hoc Dunn's test for multiple comparisons: *, P < 0.05; **, P < 0.01; ***, P < 0.001. Statistical differences remain when comparisons are made using Student's *t* test. Bar = 10 µm.

phosphatase, which has been shown to inhibit JNK activity in *Drosophila* (Ring and Martinez Arias, 1993; Martín-Blanco et al., 1998; Dobens et al., 2001). Overexpression of UAS-*puckered* has no effect on synapse stability (Fig. 8). We also find no change in synapse stability in the *wallenda* (MAPKKK) mutant background or when a dominant-negative JNK transgene is neuronally expressed (Fig. 8). From these data we conclude that inhibition of this MAPK signaling pathway does not trigger an underlying neurodegenerative response. This is consistent with the observation that Wallenda protein levels are normally maintained at low steady-state levels in *Drosophila* neurons through the activity of the ubiquitin proteosome system (Collins et al., 2006). This is also consistent with recent work in *C. elegans* where it has been shown that disruption of the homologous MAPK signaling system does not alter synapse stability (Hammarlund et al., 2009). Finally, we assayed Wnd protein levels, comparing wild-type and α-spectrin–depleted animals, examining both the ventral nerve cord and the NMJ. Wnd protein levels are kept low through the activity of the ubiquitin-proteosome system and, therefore, increased Wnd function would be expected to correlate with increased Wnd protein (Collins et al., 2006). However, we did not find an

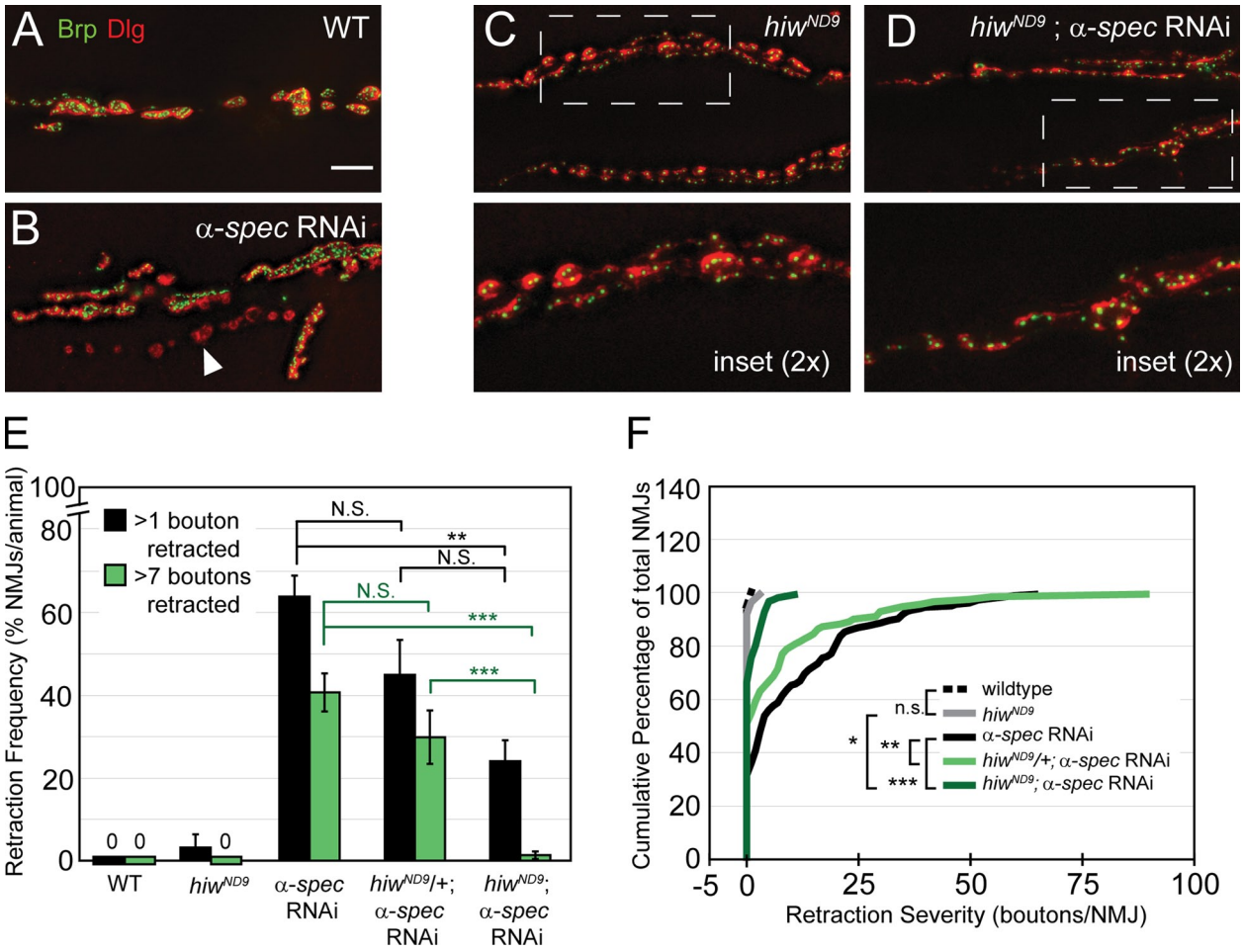

Figure 7. ***highwire* mutation suppresses synaptic instability at the NMJ.** (A–D) Representative images of muscle 6/7 NMJs stained for the presynaptic active zone protein Brp (green) and postsynaptic Dlg (red). (A) A wild-type NMJ. (B) An NMJ lacking presynaptic α-spectrin shows a large retraction, encompassing an entire branch (arrowhead). (C) hiw^{ND9} NMJs show altered morphology and overgrowth, but they maintain apposition of pre and postsynaptic markers and do not show a substantial amount of retractions (2x magnification of boxed region is shown below). (D) Presynaptic expression of UAS–α-*spectrin*–dsRNA in homozygous hiw^{ND9} mutants results in a much abrogated frequency and severity of synaptic retractions as compared with expression in a wild-type background. hiw^{ND9} NMJs that lack presynaptic α-spectrin show a characteristic hiw^{ND9} morphology and maintain good apposition of pre and postsynaptic markers (2x magnification of boxed region is shown below). (E and F) Quantification of retraction frequency (E) is plotted as the average percentage of NMJs with >1 or >7 boutons retracted. Retraction severity (F) is measured as the number of boutons per NMJ that are retracted and the data are plotted as a cumulative frequency histogram for each genotype. Wild type = w^{1118} (n = 70 NMJs/7 animals). hiw^{ND9} = hiw^{ND9}/ hiw^{ND9} or hiw^{ND9}/Y (n = 65 NMJs/7 animals). α-*spec* RNAi = $elav^{C155}$-GAL4/+ or $elav^{C155}$-GAL4/Y; 2x UAS–α-*spectrin*–dsRNA (n = 182 NMJs/19 animals). hiw^{ND9}/+; α-*spec* RNAi; = $elav^{C155}$-GAL4, hiw^{ND9}/+; 2x UAS–α-*spectrin*–dsRNA (n = 106 NMJs/11 animals). hiw^{ND9}; α-*spec* RNAi; = $elav^{C155}$-GAL4, hiw^{ND9}/Y; 2x UAS–α-*spectrin*–dsRNA (n = 149 NMJs/15 animals). Error bars represent SEM; P values for retraction frequency were determined using one-way ANOVA with post-hoc Tukey-Kramer; P values for retraction severity were determined using a Kruskal-Wallis test with a post-hoc Dunn's test for multiple comparisons: *, P < 0.05; **, P < 0.01; ***, P < 0.001. Statistical differences remain when comparisons are made with Student's *t* test. Bar = 10 µm.

induction of Wnd protein. This suggests that cytoskeletal disruption induces a neuronal stress response that is independent or downstream of Wnd.

In contrast to Wnd, Fos protein is maintained at detectable levels in neurons as assayed by Western blot, and there is endogenous activity of a Fos reporter, suggesting that Fos is constitutively active in neurons. Therefore, we next tested whether Fos is necessary for NMJ stability during normal development. Existing *fos* null mutants are embryonic lethal. Therefore, to assess a potential required function of *fos* during NMJ stability, we first assayed a heterozygous *fos* null mutant (*kayak*/+) that reduces protein levels and Fos activity by 50% (Figs. 5 and 8). These heterozygous mutants survive to be normally sized third-instar larvae and we find no change in synapse stability compared with wild type.

We next assayed a hypomorphic *fos* mutation that survives until mid-larval stages. We assayed NMJ stability at the second-instar stage and found no evidence of NMJ degeneration. However, we have previously shown that NMJ degeneration after loss of *ankyrin2-L* is a progressive process such that second-instar animals show relatively few retractions and retraction frequency increases significantly over the ensuing 2 d of larval development (Pielage et al., 2008). Therefore, we aged second-instar *fos* hypomorphic mutants for an additional 3 d before assaying the NMJ for degeneration. The *fos* hypomorphic mutations survive for at least 3 d as growth arrested second-instar larvae. Again, we found no evidence of NMJ degeneration in aged second-instar *fos* mutant larvae. These data suggest that *fos* is not critically required for NMJ stability, but

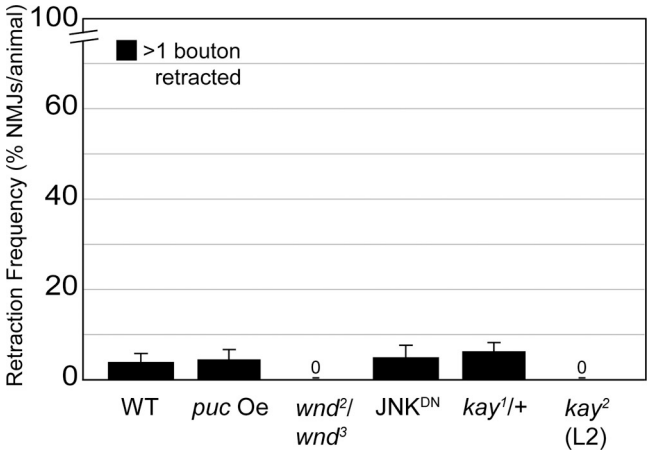

Figure 8. **Wnd/JNK signaling is not required for stability.** Retraction frequency is quantified for multiple genetic manipulations of MAPK signaling. Quantification of retraction frequency is measured as the average percentage of NMJs with >1 bouton retracted. puc Oe = *elav*^{C155}-GAL4/+; UAS-*puc* (n = 97 NMJs/10 animals). *wnd*^{2}/*wnd*^{3} (n = 105 NMJs/11 animals). JNK^{DN} = *elav*^{C155}-GAL4/+; UAS-*JNK*^{DN} (n = 108 NMJs/11 animals). *kay*^{1}/+ (n = 118 NMJs/12 animals). *kay*^{2}(L2) (n = 72 NMJs/9 animals). Error bars represent SEM. Neither one-way ANOVA nor Student's t test determined any significant differences in mean retraction frequency between genotypes.

it remains possible that residual Fos activity is sufficient for synapse stability in these experiments or that NMJ disassembly occurs only during the late stages of larval neuromuscular growth and development.

Discussion

Here we define genetic and transgenic conditions capable of conferring enhanced NMJ stability after the loss of presynaptic α-spectrin, a molecule that is necessary for normal microtubule organization and which has been termed a master organizer of the cell membrane (Lacas-Gervais et al., 2004). Enhanced NMJ stability in the absence of spectrin suggests that NMJ destabilization and degeneration are not simply a catastrophic collapse of the NMJ, but might be mediated through additional signaling processes. Consistent with this hypothesis, we show a molecular link to Wallerian-type degeneration. These advances could provide insight into the molecular processes underlying neural degeneration caused by spectrin mutations in vertebrate model systems and humans (Parkinson et al., 2001; LaMonte et al., 2002; Hafezparast et al., 2003; Puls et al., 2003; Ligon et al., 2005; Ikeda et al., 2006; Levy et al., 2006; Bennett and Healy, 2008).

We then go on to define a molecular pathway that appears to be centrally involved in the degenerative process at this synapse. We have documented a sequence of events that occur after a persistent cytoskeletal disruption. We demonstrate that an acute cytoskeletal perturbation causes a transient induction of the immediate early gene *fos*. Because transgenic expression of Fos is sufficient to suppress synapse retraction in this system, we suggest that the transient elevation of Fos represents an initial stabilizing response. We then provide evidence that elevated Fos activates a negative feedback loop by increasing the transcription of the dual specificity phosphatase *puckered*. The induction of Puckered-dependent negative feedback is delayed relative to the stabilizing increase in Fos and is observed to persist throughout the life of the larvae. Thus, our data suggest that during a prolonged cytoskeletal perturbation, transient stabilizing Fos activity is replaced by a strong induction of *puckered*. The induction of *puckered* has been shown to suppress baseline JNK/Fos activity and should, therefore, prevent reactivation of stabilizing Fos signaling during a persistent cellular stress. The delayed activation of Puckered-dependent negative feedback in the presence of a persistent cytoskeletal stress could represent an endogenous mechanism to ensure that Fos activity is inhibited in the presence of ongoing stress and switch the motoneuron into a state that favors rapid NMJ retraction. Such a system would favor synapse stability when it is possible to repair cellular damage, but favor the elimination of a neuron when damage persists.

This model predicts that prolonging Fos expression or inhibiting Puckered transcription should prolong synapse stability despite the presence of a persistent cytoskeletal disruption (Fig. 9). This is precisely what we observe. In addition, loss of function mutation in the E3 ubiquitin ligase *highwire*, which is believed to potentiate baseline Fos signaling (Collins et al., 2006), also significantly suppresses NMJ retraction (Fig. 9).

The next question we considered was whether the cellular state represented by low Fos/high Puckered activity causes synapse loss, or whether this state permits the expression of a destabilizing process during persistent cellular stress. In principle, overexpression of UAS-*puckered* should mimic the low Fos/high Puckered signaling state. When we overexpressed UAS-*puckered* pan-neuronally we found no change in NMJ stability. Thus, it seems that this pathway permits the induction of a destabilizing process rather than directly inducing disassembly.

The model for a temporal switch from stabilization to disassembly shares similarity to a model for stress-induced cell death that involves the induction of the unfolded protein response (UPR) (Lin et al., 2007). The UPR can elicit both a protective response by reestablishing appropriate levels of unfolded protein as well as pro-apoptic signaling. A recent study has provided evidence that the switch from protective to pro-apoptotic signaling correlates with the duration of activation for different signaling systems downstream of UPR induction. All downstream signaling systems are initially induced, but the switch to pro-apoptotic signaling is correlated with the decay of IRE1 signaling and the prolonged activation of PERK signaling (Lin et al., 2007). Again, the switch from protective to cell-destructive signaling is achieved by temporal changes in the balance of signaling systems that reside downstream of a persistent cellular stress.

Sustaining motoneuron integrity despite loss of presynaptic α-spectrin

We previously demonstrated that loss of presynaptic α-spectrin causes profound synaptic loss at the NMJ (Pielage et al., 2005). Impaired NMJ stability was correlated with the loss of synaptic cell adhesion, a severely disorganized microtubule cytoskeleton, and the appearance of large protein aggregations in motor axons (Pielage et al., 2005). It is remarkable, therefore, that increased expression of Wld^{S}, Gbb, or Fos can

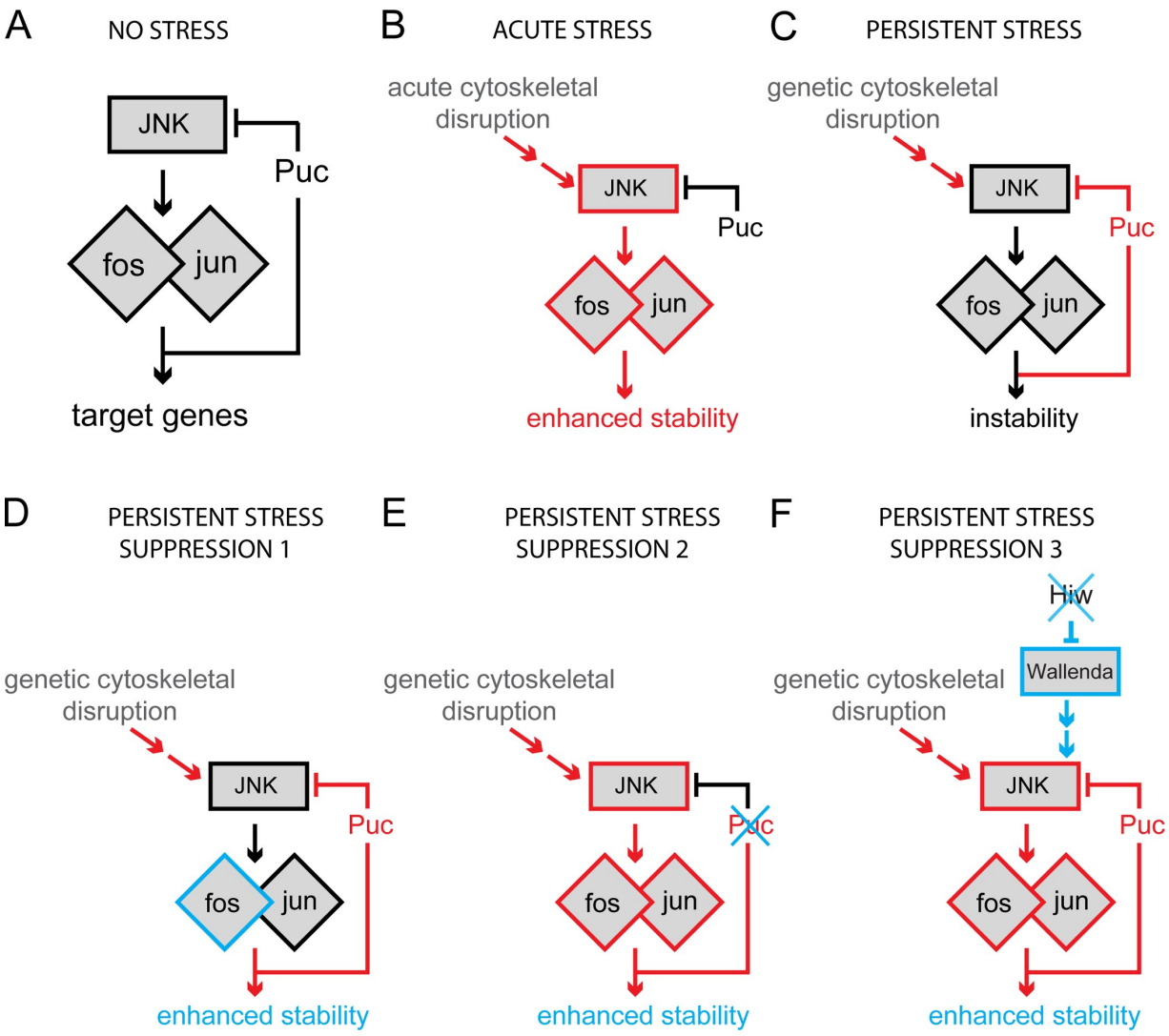

Figure 9. **Model for synapse stabilizing effects of MAPK signaling.** (A–C) Effects of stress on MAPK signaling. (A) In the absence of cellular stress this JNK-Fos pathway is at steady state (shown in black) and is not necessary for endogenous synapse stability. (B) Acute cellular stress (e.g., cytoskeletal disruption) induces activation (shown in red) of JNK and Fos, which enhances synapse stabilization. The elevation of Fos is transient. (C) In the presence of a persistent cellular stress, negative feedback via the phosphatase Puckered prevents reactivation of Fos and the neuron switches toward a state that favors disassembly or instability. (D–F) Experimental manipulations (shown in blue) that result in enhanced synapse stability in the presence of a persistent cellular stress. (D) Fos overexpression results in enhanced stability. (E) Loss of Puckered-dependent feedback inhibition promotes synapse stability, likely through enhanced Fos activity. (F) Loss of Highwire potentiates upstream MAPK signaling, acting through Fos to promote synapse stability.

significantly preserve synapse stability in animals that lack presynaptic α-spectrin.

Several studies have documented a neuroprotective effect of synaptic growth. Increased expression of CNTF is neuroprotective in a mouse model of ALS (Pun et al., 2006). It was also shown that NMJs with an increased endogenous capacity for synaptic growth and remodeling are more resistant to degeneration in a mouse model of ALS (Frey et al., 2000; Pun et al., 2006). Consistent with the importance of growth factor signaling, we show that Gbb overexpression is able to rescue synapse stability. However, overexpression of Wld^S or UAS-*fos* has no effect on synaptic growth (Sanyal et al., 2002; unpublished data). In addition, a heterozygous *highwire* mutation is sufficient to rescue some aspects of synapse stability in animals that lack presynaptic α-spectrin without stimulating significant NMJ growth (Fig. 7). Therefore, although the stabilizing function of Wld^S or Fos may be related to the mechanisms that are required for synaptic growth (Collins et al., 2006), enhanced NMJ growth is not necessary for the stabilizing actions of Fos.

We considered the possibility that loss of spectrin causes motor axons to break, followed by a neurodegenerative response. The basis for this consideration is the recent demonstration that loss of spectrin in *C. elegans* causes motor axons to break during animal motility (Hammarlund et al., 2007, 2009). In *Drosophila*, it does not appear that motor axons break after loss of neuronal spectrin. It was previously shown that the severity of NMJ degeneration precisely correlates with the disruption of synaptic transmission at the NMJ (Pielage et al., 2005). Specifically, a small degenerative event that encompasses ~25% of the NMJ was not associated with any defect in synaptic transmission, whereas a degenerative event encompassing >60% of the NMJ was associated with a significant decrease in

synaptic transmission. However, in both cases, the presynaptic action potentials clearly invade the presynaptic nerve terminal and reliably evoke neurotransmitter release. This would not be the case if there were axonal breaks. It is interesting, however, that MAPK signaling is emerging as an important pathway involved in axon regeneration (Ayaz et al., 2008; Hammarlund et al., 2009) and, as shown here, the transition from stabilization to disassembly at the NMJ.

Finally, a recently published study provides evidence that Wallenda and JNK function specifically in distal neuronal processes, severed from the neuronal soma, to promote Wallerian-type degeneration (Miller et al., 2009). These recent data are in apparent contrast with the neuronal growth-promoting function of Wallenda/JNK/Fos during neural development (Wan et al., 2000; DiAntonio et al., 2001; Sanyal et al., 2002; Collins et al., 2006) and axon regeneration (Hammarlund et al., 2009). Furthermore, previous studies have shown that both Wallenda and JNK normally promote axonal transport, which is required for ongoing neuronal health (Byrd et al., 2001; Horiuchi et al., 2007). One possible way to reconcile these recent data from Miller et al. (2009) with our current model is to consider the cellular compartment in which the signaling pathways have been examined. In an intact cell, MAPK/JNK/Fos signaling appears to generally promote synapse stability, axonal transport, cell growth, and neuroprotection. In contrast, within an axonal process that has been severed from the cell body and is destined to degenerate, Wallenda and JNK may function to facilitate the induction of the degenerative process. Thus, there may be context-dependent and compartment-specific functions of this important, stress response pathway.

Materials and methods

Fly stocks

Flies were maintained at 25°C on normal food, unless otherwise noted. The following strains were used in the study: w^{1118} (wild type), $elav^{C155}$-GAL4 (neuron-specific; Lin and Goodman, 1994), *BG57*-GAL4 (muscle specific; Budnik et al., 1996), hiw^{ND9} (Wan et al., 2000), puc^{1} and $puc^{A251.1F3}$ (Martín-Blanco et al., 1998), wnd^{2} and wnd^{3} (Collins et al., 2006), kay^{1}(Riesgo-Escovar and Hafen, 1997), kay^{2} (courtesy of D. Bohmann, University of Rochester, Rochester, NY), GAL4-responsive UAS-Wld^{s} (Hoopfer et al., 2006), UAS-*gbb* (S. Thor, University of Cambridge, Cambridge, UK; Wharton et al., 1999), UAS-*puc* (Martín-Blanco et al., 1998), UAS-*fos* and UAS-*jun*, (Eresh et al., 1997) UAS-bsk^{DN} (Weber et al., 2000), UAS–α-*spectrin*–dsRNA (Pielage et al., 2005), $Pbac(WH)CG32373^{f02001}$ [P($CG32373^{2001}$) or $ank2^{2001}$] (identified in the BDGP/Exelixis gene disruption project), and Df(3L)RM5-2 (from the Bloomington stock center, Bloomington, IN). All UAS constructs were driven presynaptically with $elav^{C155}$-GAL4, except for Fig. 1 (D and E), where UAS constructs were simultaneously driven both presynaptically with $elav^{C155}$-GAL4 and postsynaptically with *BG57*-GAL4.

Throughout this paper we make use of multiple genomic insertions of the UAS–α-*spectrin* RNAi transgene. To allow for construction of double mutants in different experiments, either one or two copies of the RNAi transgene were used. This results in different baseline retraction phenotypes in different experiments, with a single copy of the RNAi transgene causing a lower frequency and severity of retractions than the two copies. The milder phenotype seen with a single copy of UAS–α-*spectrin* RNAi is significantly different from wild type, and is qualitatively identical to the more severe phenotype seen with two copies of UAS–α-*spectrin* RNAi. One copy of UAS–α-*spectrin* RNAi was used in the following figures: Fig. 4 (F and G) and Fig. 6. Two copies of UAS–α-*spectrin* RNAi were used in the following figures: Figs. 1, 2, 3, 4 (A–E), 5, and 7, and S1–S3.

Immunocytochemistry and imaging

Wandering third-instar larvae were dissected in HL3 saline (Stewart et al., 1994) and fixed in Bouin's fixative (Sigma-Aldrich). Primary antibodies were applied at 4°C overnight. Primary antibodies were used at the following dilutions: anti-bruchpilot, 1:50; anti-Futsch, 1:20; anti-α-spectrin, 1:20; anti-Fasciclin II, 1:10; anti-Neuroglian, 1:10 (all provided by the Developmental Studies Hybridoma Bank, Iowa City, IA); rabbit anti–Wallenda, 1:100 (courtesy of A. DiAntonio, Washington University, St. Loius, MO); anti–β-Galactosidase, 1:50 (Cell Signaling Technology); and rabbit polyclonal anti-Dlg, 1:10,000 (Budnik et al., 1996). Secondary Alexa Fluor antibodies (goat anti–mouse 488, goat anti–rabbit 555, and goat anti–rabbit 647) were obtained from Invitrogen and used at a 1:600 dilution. All other secondary antibodies and Cy3-conjugated HRP were obtained from Jackson Immunoresearch Laboratories, Inc. or Invitrogen and used at a 1:200 dilution. All secondary antibodies were applied for 1–2 h at room temperature. All NMJ image stacks were captured using an inverted microscope (Axiovert 200; Carl Zeiss, Inc.) with a Plan-APOCHROMAT 100x oil-immersion lens (NA = 1.40; Carl Zeiss, Inc.), a cooled CCD camera (CoolSnapHQ; Photometrics), and piezo controlled z-axis positioning. All images were taken at room temperature, using Immersol imaging oil (Carl Zeiss, Inc.). Hardware and software analysis was driven by Intelligent Imaging Innovations (3I) software, specifically the Slidebook imaging program. Using the Slidebook software, images were deconvolved with the nearest neighbor algorithm, and z-stacks were combined into a single projection image. Further processing of images, specifically cropping and adjustment of levels, was done in Adobe Photoshop. No thresholding was incorporated into the images shown. Ventral nerve cord image stacks (Fig. 5 D) were captured using a microscope (Axioskop 2; Carl Zeiss, Inc.) and the LSM 510 Meta Laser Scanning System (Carl Zeiss, Inc.). Images were acquired with a Plan-APOCHROMAT 40x oil-immersion lens (NA = 1.3; Carl Zeiss, Inc.), a CCD camera (Rolera-XR Mono Fast 1394; QImaging) and piezo controlled z-axis positioning. All images were taken at room temperature, using Immersol imaging oil (Carl Zeiss, Inc.). Hardware and software analysis was driven by LSM 510 software (Carl Zeiss, Inc.). Using the LSM 510 software, z-stacks were combined into a single projection image, and further processing of images, specifically cropping and adjustment of levels, was done in Adobe Photoshop.

Image quantification

All retractions were counted at 40x magnification, and the observer was blind to genotype. Segments A2 through A6 were counted. A retraction was defined as an area of the NMJ where clearly defined postsynaptic Dlg staining is not apposed by presynaptic nc82 staining. Levels of immunoreactivity were quantified (Figs. 1 and S3) using the masking function in Slidebook. Image stacks were taken at the same exposure from animals that were dissected and stained together. Images were deconvolved and projected into a single 3D stack before masking. No alterations were made to the images before quantification.

Electrophysiology

Recordings were performed as described previously (Albin and Davis, 2004). Specifically, wandering third-instar larvae were selected after leaving the food. Larvae were recorded in HL3 saline with 0.3 mM Ca^{2+} and 10 mM Mg^{2+}. Muscle recordings were made from muscle 6 in abdominal segment 3 (A3) and were achieved using sharp electrodes (12–18 MΩ) filled with 3M potassium chloride. Stimulation electrodes were fabricated with an opening equal to the diameter of the motor nerve. Stimulation threshold was set for each recording such that the maximal EPSP was achieved, including the recruitment of both motoneurons contacting muscle 6. Recordings were performed using an Axoclamp2B amplifier (Axon Instruments), Master-8 stimulator (AMPI) and digitized using Axon Instruments hardware and P-Clamp software (Axon Instruments). Electrodes were positioned using MP285 micromanipulators (Sutter Instrument Co.). All recordings were made in current clamp mode and analyzed offline. The preparation was visualized using a compound, fixed stage microscope (model BX50WI; Olympus) and 40x water immersion lens (0.8 NA). Quantal content was calculated by dividing the average maximal EPSP amplitude by the average amplitude of the spontaneous miniature release events (mEPSP) for each recording. Multiple recordings were averaged per genotype. Measurements of maximal EPSP and input resistance were done by hand using the cursor option in Clampfit (MDS Analytical Technologies). Measurements of spontaneous miniature release events were semi-automated using MiniAnalysis software (Synaptosoft). For each recording, 100–300 mEPSP events were averaged to determine the average mEPSP amplitude.

β-Gal activity assay

β-Galactosidase activity was measured using the Glacto-Light Plus System (Applied Biosystems). Samples consisted of at least three animals for each condition, and all assays were conducted in duplicate. For genetics experiments (i.e., comparisons between animals of different genotype), animals were dissected in HL3 saline with 0 mM Ca^{2+} and 20 mM Mg^{2+}, and then transferred to lysis buffer for homogenization immediately after dissection. For nocodazole experiments, animals were dissected in HL3 saline with 0.5 mM Ca^{2+} and 10 mM Mg^{2+}, and then incubated for 30 min, 1 h, 2 h, or 4 h in identical HL3 solution with nocodazole in DMSO or DMSO only (control condition). After incubation, animals were transferred to lysis buffer for homogenization. A standard Bradford assay for protein concentration was performed on each sample, and β-Galactosidase activity was normalized to within-sample protein concentration for each condition.

Western blotting

For genetics experiments (i.e., comparisons between animals of different genotype), animals were dissected in HL3 saline with 0 mM Ca^{2+} and 20 mM Mg^{2+}. The CNS was removed from each animal and homogenized in sample buffer (95% 2x Laemmli sample buffer with 5% 2-Mercaptoethanol). For nocodazole experiments, animals were dissected in HL3 saline with 0.5 mM Ca^{2+} and 10 mM Mg^{2+}, and then incubated for 30 min or 2 h in identical HL3 solution with nocodazole in DMSO or DMSO only (control condition). After incubation, the CNS was removed from each animal and homogenized in sample buffer. Samples consisted of at least five CNS for each condition. Samples were boiled for 15 min and then run on 7.5% tris-HCl gels at 35 mA. Gels were transferred to PVDF membrane for 1 h at 100 V, and then membranes were probed with one of two rabbit anti-Fos antibodies (101AP from Fabgennix, Inc., or courtesy of D. Bohmann) at 1:1,000. Secondary antibody (goat anti–rabbit-HRP) was obtained from Jackson Immunoresearch Laboratories, Inc., and used at 1:5,000. To control for protein loading, membranes were stripped with Restore Western Blot Stripping Buffer (Thermo Fisher Scientific) and reprobed with mouse anti-β-tubulin (courtesy of U. Heberlein, University of California, San Francisco, San Francisco, CA) at 1:1,000 or mouse anti-actin (Sigma-Aldrich) at 1:10,000. Secondary antibody (goat anti–mouse-HRP) was obtained from Jackson Immunoresearch Laboratories, Inc., and used at 1:10,000. All antibody incubations were done at room temperature for 1 h in 2% milk in TBS with 0.1% Tween 20. All membranes were developed with ECL substrate (GE Healthcare) and exposed to film. Films were quantified with the ImageJ gel analysis tool (National Institutes of Health, Bethesda, MD).

Online supplemental material

Fig. S1 provides evidence that neuronal expression of *α-spectrin* RNAi eliminates presynaptic α-spectrin protein from the nerve at the neuromuscular junction. Fig. S2 provides evidence that expression of UAS-*fos* suppresses synaptic retraction in the *ankyrin2-L* mutant background. Fig. S3 demonstrates that the levels of two prominent synaptic cell adhesion molecules, Fasciclin II and Neuroglian, are not significantly increased by neuronal expression UAS-*fos*. Online supplemental material is available at http://www.jcb.org/cgi/content/full/jcb.200903166/DC1.

This work was supported by the Training Grant for Neurodegenerative Diseases and an Achievement Rewards for College Scientists scholarship to C.M. Massaro, and National Institutes of Health grant NS047342 to G.W. Davis.

Submitted: 31 March 2009
Accepted: 8 September 2009

References

Aberle, H., A.P. Haghighi, R.D. Fetter, B.D. McCabe, T.R. Magalhães, and C.S. Goodman. 2002. *wishful thinking* encodes a BMP type II receptor that regulates synaptic growth in *Drosophila*. *Neuron.* 33:545–558. doi:10.1016/S0896-6273(02)00589-5

Agnès, F., M. Suzanne, and S. Noselli. 1999. The *Drosophila* JNK pathway controls the morphogenesis of imaginal discs during metamorphosis. *Development.* 126:5453–5462.

Albin, S.D., and G.W. Davis. 2004. Coordinating structural and functional synapse development: postsynaptic p21-activated kinase independently specifies glutamate receptor abundance and postsynaptic morphology. *J. Neurosci.* 24:6871–6879. doi:10.1523/JNEUROSCI.1538-04.2004

Avery, M.A., A.E. Sheehan, K.S. Kerr, J. Wang, and M.R. Freeman. 2009. Wld S requires Nmnat1 enzymatic activity and N16-VCP interactions to suppress Wallerian degeneration. *J. Cell Biol.* 184:501–513. doi:10.1083/jcb.200808042

Ayaz, D., M. Leyssen, M. Koch, J. Yan, M. Srahna, V. Sheeba, K.J. Fogle, T.C. Holmes, and B.A. Hassan. 2008. Axonal injury and regeneration in the adult brain of *Drosophila*. *J. Neurosci.* 28:6010–6021. doi:10.1523/JNEUROSCI.0101-08.2008

Bennett, V., and J. Davis. 1983. Spectrin and ankyrin in brain. *Cell Motil.* 3:623–633. doi:10.1002/cm.970030527

Bennett, V., and D.M. Gilligan. 1993. The spectrin-based membrane skeleton and micron-scale organization of the plasma membrane. *Annu. Rev. Cell Biol.* 9:27–66. doi:10.1146/annurev.cb.09.110193.000331

Bennett, V., and J. Healy. 2008. Organizing the fluid membrane bilayer: diseases linked to spectrin and ankyrin. *Trends Mol. Med.* 14:28–36. doi:10.1016/j.molmed.2007.11.005

Bennett, V., and S. Lambert. 1991. The spectrin skeleton: from red cells to brain. *J. Clin. Invest.* 87:1483–1489. doi:10.1172/JCI115157

Budnik, V., Y.H. Koh, B. Guan, B. Hartmann, C. Hough, D. Woods, and M. Gorczyca. 1996. Regulation of synapse structure and function by the *Drosophila* tumor suppressor gene dlg. *Neuron.* 17:627–640. doi:10.1016/S0896-6273(00)80196-8

Byrd, D.T., M. Kawasaki, M. Walcoff, N. Hisamoto, K. Matsumoto, and Y. Jin. 2001. UNC-16, a JNK-signaling scaffold protein, regulates vesicle transport in *C. elegans*. *Neuron.* 32:787–800. doi:10.1016/S0896-6273(01)00532-3

Cho, S., E.M. Park, Y. Kim, N. Liu, J. Gal, B.T. Volpe, and T.H. Joh. 2001. Early c-Fos induction after cerebral ischemia: a possible neuroprotective role. *J. Cereb. Blood Flow Metab.* 21:550–556. doi:10.1097/00004647-200105000-00009

Collins, C.A., Y.P. Wairkar, S.L. Johnson, and A. DiAntonio. 2006. Highwire restrains synaptic growth by attenuating a MAP kinase signal. *Neuron.* 51:57–69. doi:10.1016/j.neuron.2006.05.026

Conforti, L., A. Wilbrey, G. Morreale, L. Janeckova, B. Beirowski, R. Adalbert, F. Mazzola, M. Di Stefano, R. Hartley, E. Babetto, et al. 2009. Wld S protein requires Nmnat activity and a short N-terminal sequence to protect axons in mice. *J. Cell Biol.* 184:491–500. doi:10.1083/jcb.200807175

DiAntonio, A., A.P. Haghighi, S.L. Portman, J.D. Lee, A.M. Amaranto, and C.S. Goodman. 2001. Ubiquitination-dependent mechanisms regulate synaptic growth and function. *Nature.* 412:449–452. doi:10.1038/35086595

Dobens, L.L., E. Martín-Blanco, A. Martínez-Arias, F.C. Kafatos, and L.A. Raftery. 2001. *Drosophila* puckered regulates Fos/Jun levels during follicle cell morphogenesis. *Development.* 128:1845–1856.

Dragunow, M., E. Beilharz, E. Sirimanne, P. Lawlor, C. Williams, R. Bravo, and P. Gluckman. 1994. Immediate-early gene protein expression in neurons undergoing delayed death, but not necrosis, following hypoxic-ischaemic injury to the young rat brain. *Brain Res. Mol. Brain Res.* 25:19–33. doi:10.1016/0169-328X(94)90274-7

Eaton, B.A., and G.W. Davis. 2005. LIM Kinase1 controls synaptic stability downstream of the type II BMP receptor. *Neuron.* 47:695–708. doi:10.1016/j.neuron.2005.08.010

Eaton, B.A., R.D. Fetter, and G.W. Davis. 2002. Dynactin is necessary for synapse stabilization. *Neuron.* 34:729–741. doi:10.1016/S0896-6273(02)00721-3

Eresh, S., J. Riese, D.B. Jackson, D. Bohmann, and M. Bienz. 1997. A CREB-binding site as a target for decapentaplegic signalling during *Drosophila* endoderm induction. *EMBO J.* 16:2014–2022. doi:10.1093/emboj/16.8.2014

Ferri, A., J.R. Sanes, M.P. Coleman, J.M. Cunningham, and A.C. Kato. 2003. Inhibiting axon degeneration and synapse loss attenuates apoptosis and disease progression in a mouse model of motoneuron disease. *Curr. Biol.* 13:669–673. doi:10.1016/S0960-9822(03)00206-9

Fischer, L.R., D.G. Culver, A.A. Davis, P. Tennant, M. Wang, M. Coleman, S. Asress, R. Adalbert, G.M. Alexander, and J.D. Glass. 2005. The WldS gene modestly prolongs survival in the SOD1G93A fALS mouse. *Neurobiol. Dis.* 19:293–300. doi:10.1016/j.nbd.2005.01.008

Frey, D., C. Schneider, L. Xu, J. Borg, W. Spooren, and P. Caroni. 2000. Early and selective loss of neuromuscular synapse subtypes with low sprouting competence in motoneuron diseases. *J. Neurosci.* 20:2534–2542.

Hafezi, F., J.P. Steinbach, A. Marti, K. Munz, Z.Q. Wang, E.F. Wagner, A. Aguzzi, and C.E. Remé. 1997. The absence of c-fos prevents light-induced apoptotic cell death of photoreceptors in retinal degeneration in vivo. *Nat. Med.* 3:346–349. doi:10.1038/nm0397-346

Hafezparast, M., R. Klocke, C. Ruhrberg, A. Marquardt, A. Ahmad-Annuar, S. Bowen, G. Lalli, A.S. Witherden, H. Hummerich, S. Nicholson, et al. 2003. Mutations in dynein link motor neuron degeneration to defects in retrograde transport. *Science.* 300:808–812. doi:10.1126/science.1083129

Hammarlund, M., E.M. Jorgensen, and M.J. Bastiani. 2007. Axons break in animals lacking beta-spectrin. *J. Cell Biol.* 176:269–275. doi:10.1083/jcb.200611117

Hammarlund, M., P. Nix, L. Hauth, E.M. Jorgensen, and M. Bastiani. 2009. Axon regeneration requires a conserved MAP kinase pathway. *Science.* 323:802–806. doi:10.1126/science.1165527

Hoopfer, E.D., T. McLaughlin, R.J. Watts, O. Schuldiner, D.D. O'Leary, and L. Luo. 2006. Wlds protection distinguishes axon degeneration following injury from naturally occurring developmental pruning. *Neuron.* 50:883–895. doi:10.1016/j.neuron.2006.05.013

Horiuchi, D., C.A. Collins, P. Bhat, R.V. Barkus, A. Diantonio, and W.M. Saxton. 2007. Control of a kinesin-cargo linkage mechanism by JNK pathway kinases. *Curr. Biol.* 17:1313–1317. doi:10.1016/j.cub.2007.06.062

Ikeda, Y., K.A. Dick, M.R. Weatherspoon, D. Gincel, K.R. Armbrust, J.C. Dalton, G. Stevanin, A. Dürr, C. Zühlke, K. Bürk, et al. 2006. Spectrin mutations cause spinocerebellar ataxia type 5. *Nat. Genet.* 38:184–190. doi:10.1038/ng1728

Keshishian, H., K. Broadie, A. Chiba, and M. Bate. 1996. The *Drosophila* neuromuscular junction: a model system for studying synaptic development and function. *Annu. Rev. Neurosci.* 19:545–575. doi:10.1146/annurev.ne.19.030196.002553

Koch, I., H. Schwarz, D. Beuchle, B. Goellner, M. Langegger, and H. Aberle. 2008. *Drosophila* ankyrin 2 is required for synaptic stability. *Neuron.* 58:210–222. doi:10.1016/j.neuron.2008.03.019

Lacas-Gervais, S., J. Guo, N. Strenzke, E. Scarfone, M. Kolpe, M. Jahkel, P. De Camilli, T. Moser, M.N. Rasband, and M. Solimena. 2004. BetaIVSigma1 spectrin stabilizes the nodes of Ranvier and axon initial segments. *J. Cell Biol.* 166:983–990. doi:10.1083/jcb.200408007

LaMonte, B.H., K.E. Wallace, B.A. Holloway, S.S. Shelly, J. Ascaño, M. Tokito, T. Van Winkle, D.S. Howland, and E.L. Holzbaur. 2002. Disruption of dynein/dynactin inhibits axonal transport in motor neurons causing late-onset progressive degeneration. *Neuron.* 34:715–727. doi:10.1016/S0896-6273(02)00696-7

Levy, J.R., C.J. Sumner, J.P. Caviston, M.K. Tokito, S. Ranganathan, L.A. Ligon, K.E. Wallace, B.H. LaMonte, G.G. Harmison, I. Puls, et al. 2006. A motor neuron disease-associated mutation in p150Glued perturbs dynactin function and induces protein aggregation. *J. Cell Biol.* 172:733–745. doi:10.1083/jcb.200511068

Ligon, L.A., B.H. LaMonte, K.E. Wallace, N. Weber, R.G. Kalb, and E.L. Holzbaur. 2005. Mutant superoxide dismutase disrupts cytoplasmic dynein in motor neurons. *Neuroreport.* 16:533–536. doi:10.1097/00001756-200504250-00002

Lin, D.M., and C.S. Goodman. 1994. Ectopic and increased expression of Fasciclin II alters motoneuron growth cone guidance. *Neuron.* 13:507–523. doi:10.1016/0896-6273(94)90022-1

Lin, J.H., H. Li, D. Yasumura, H.R. Cohen, C. Zhang, B. Panning, K.M. Shokat, M.M. Lavail, and P. Walter. 2007. IRE1 signaling affects cell fate during the unfolded protein response. *Science.* 318:944–949. doi:10.1126/science.1146361

Lonze, B.E., A. Riccio, S. Cohen, and D.D. Ginty. 2002. Apoptosis, axonal growth defects, and degeneration of peripheral neurons in mice lacking CREB. *Neuron.* 34:371–385. doi:10.1016/S0896-6273(02)00686-4

Luo, L., and D.D. O'Leary. 2005. Axon retraction and degeneration in development and disease. *Annu. Rev. Neurosci.* 28:127–156. doi:10.1146/annurev.neuro.28.061604.135632

Lyon, M.F., B.W. Ogunkolade, M.C. Brown, D.J. Atherton, and V.H. Perry. 1993. A gene affecting Wallerian nerve degeneration maps distally on mouse chromosome 4. *Proc. Natl. Acad. Sci. USA.* 90:9717–9720. doi:10.1073/pnas.90.20.9717

Mabuchi, T., K. Kitagawa, K. Kuwabara, K. Takasawa, T. Ohtsuki, Z. Xia, D. Storm, T. Yanagihara, M. Hori, and M. Matsumoto. 2001. Phosphorylation of cAMP response element-binding protein in hippocampal neurons as a protective response after exposure to glutamate in vitro and ischemia in vivo. *J. Neurosci.* 21:9204–9213.

Mack, T.G., M. Reiner, B. Beirowski, W. Mi, M. Emanuelli, D. Wagner, D. Thomson, T. Gillingwater, F. Court, L. Conforti, et al. 2001. Wallerian degeneration of injured axons and synapses is delayed by a Ube4b/Nmnat chimeric gene. *Nat. Neurosci.* 4:1199–1206. doi:10.1038/nn770

Mantamadiotis, T., T. Lemberger, S.C. Bleckmann, H. Kern, O. Kretz, A. Martin Villalba, F. Tronche, C. Kellendonk, D. Gau, J. Kapfhammer, et al. 2002. Disruption of CREB function in brain leads to neurodegeneration. *Nat. Genet.* 31:47–54. doi:10.1038/ng882

Martín-Blanco, E., A. Gampel, J. Ring, K. Virdee, N. Kirov, A.M. Tolkovsky, and A. Martinez-Arias. 1998. *puckered* encodes a phosphatase that mediates a feedback loop regulating JNK activity during dorsal closure in *Drosophila. Genes Dev.* 12:557–570. doi:10.1101/gad.12.4.557

McCabe, B.D., S. Hom, H. Aberle, R.D. Fetter, G. Marques, T.E. Haerry, H. Wan, M.B. O'Connor, C.S. Goodman, and A.P. Haghighi. 2004. Highwire regulates presynaptic BMP signaling essential for synaptic growth. *Neuron.* 41:891–905. doi:10.1016/S0896-6273(04)00073-X

Miller, B.R., C. Press, R.W. Daniels, Y. Sasaki, J. Milbrandt, and A. DiAntonio. 2009. A dual leucine kinase-dependent axon self-destruction program promotes Wallerian degeneration. *Nat. Neurosci.* 12:387–389. doi:10.1038/nn.2290

Nakata, K., B. Abrams, B. Grill, A. Goncharov, X. Huang, A.D. Chisholm, and Y. Jin. 2005. Regulation of a DLK-1 and p38 MAP kinase pathway by the ubiquitin ligase RPM-1 is required for presynaptic development. *Cell.* 120:407–420. doi:10.1016/j.cell.2004.12.017

Palop, J.J., B. Jones, L. Kekonius, J. Chin, G.Q. Yu, J. Raber, E. Masliah, and L. Mucke. 2003. Neuronal depletion of calcium-dependent proteins in the dentate gyrus is tightly linked to Alzheimer's disease-related cognitive deficits. *Proc. Natl. Acad. Sci. USA.* 100:9572–9577. doi:10.1073/pnas.1133381100

Parkinson, N.J., C.L. Olsson, J.L. Hallows, J. McKee-Johnson, B.P. Keogh, K. Noben-Trauth, S.G. Kujawa, and B.L. Tempel. 2001. Mutant beta-spectrin 4 causes auditory and motor neuropathies in quivering mice. *Nat. Genet.* 29:61–65. doi:10.1038/ng710

Parson, S.H., C.L. Mackintosh, and R.R. Ribchester. 1997. Elimination of motor nerve terminals in neonatal mice expressing a gene for slow wallerian degeneration (C57BL/Wlds). *Eur. J. Neurosci.* 9:1586–1592. doi:10.1111/j.1460-9568.1997.tb01516.x

Perry, V.H., E.R. Lunn, M.C. Brown, S. Cahusac, and S. Gordon. 1990. Evidence that the rate of Wallerian degeneration is controlled by a single autosomal dominant gene. *Eur. J. Neurosci.* 2:408–413. doi:10.1111/j.1460-9568.1990.tb00433.x

Perry, V.H., M.C. Brown, and E.R. Lunn. 1991. Very slow retrograde and Wallerian degeneration in the CNS of C57BL/Ola mice. *Eur. J. Neurosci.* 3:102–105. doi:10.1111/j.1460-9568.1991.tb00815.x

Pielage, J., R.D. Fetter, and G.W. Davis. 2005. Presynaptic spectrin is essential for synapse stabilization. *Curr. Biol.* 15:918–928. doi:10.1016/j.cub.2005.04.030

Pielage, J., L. Cheng, R.D. Fetter, P.M. Carlton, J.W. Sedat, and G.W. Davis. 2008. A presynaptic giant ankyrin stabilizes the NMJ through regulation of presynaptic microtubules and transsynaptic cell adhesion. *Neuron.* 58:195–209. doi:10.1016/j.neuron.2008.02.017

Puls, I., C. Jonnakuty, B.H. LaMonte, E.L. Holzbaur, M. Tokito, E. Mann, M.K. Floeter, K. Bidus, D. Drayna, S.J. Oh, et al. 2003. Mutant dynactin in motor neuron disease. *Nat. Genet.* 33:455–456. doi:10.1038/ng1123

Pun, S., A.F. Santos, S. Saxena, L. Xu, and P. Caroni. 2006. Selective vulnerability and pruning of phasic motoneuron axons in motoneuron disease alleviated by CNTF. *Nat. Neurosci.* 9:408–419. doi:10.1038/nn1653

Riesgo-Escovar, J.R., and E. Hafen. 1997. Common and distinct roles of DFos and DJun during *Drosophila* development. *Science.* 278:669–672. doi:10.1126/science.278.5338.669

Ring, J.M., and A. Martinez Arias. 1993. *puckered*, a gene involved in position-specific cell differentiation in the dorsal epidermis of the *Drosophila* larva. *Dev. Suppl.* 119:251–259.

Sajadi, A., B.L. Schneider, and P. Aebischer. 2004. Wlds-mediated protection of dopaminergic fibers in an animal model of Parkinson disease. *Curr. Biol.* 14:326–330.

Sanyal, S., D.J. Sandstrom, C.A. Hoeffer, and M. Ramaswami. 2002. AP-1 functions upstream of CREB to control synaptic plasticity in *Drosophila. Nature.* 416:870–874. doi:10.1038/416870a

Saura, C.A., S.Y. Choi, V. Beglopoulos, S. Malkani, D. Zhang, B.S. Shankaranarayana Rao, S. Chattarji, R.J. Kelleher III, E.R. Kandel, K. Duff, et al. 2004. Loss of presenilin function causes impairments of memory and synaptic plasticity followed by age-dependent neurodegeneration. *Neuron.* 42:23–36. doi:10.1016/S0896-6273(04)00182-5

Schuster, C.M., G.W. Davis, R.D. Fetter, and C.S. Goodman. 1996. Genetic dissection of structural and functional components of synaptic plasticity. II. Fasciclin II controls presynaptic structural plasticity. *Neuron.* 17:655–667. doi:10.1016/S0896-6273(00)80198-1

Stewart, B.A., H.L. Atwood, J.J. Renger, J. Wang, and C.F. Wu. 1994. Improved stability of *Drosophila* larval neuromuscular preparations in haemolymph-like physiological solutions. *J. Comp. Physiol. [A].* 175:179–191. doi:10.1007/BF00215114

Walton, M., G. MacGibbon, D. Young, E. Sirimanne, C. Williams, P. Gluckman, and M. Dragunow. 1998. Do c-Jun, c-Fos, and amyloid precursor protein play a role in neuronal death or survival? *J. Neurosci. Res.* 53:330–342. doi:10.1002/(SICI)1097-4547(19980801)53:3<330::AID-JNR7>3.0.CO;2-B

Walton, M., B. Connor, P. Lawlor, D. Young, E. Sirimanne, P. Gluckman, G. Cole, and M. Dragunow. 1999a. Neuronal death and survival in two models of hypoxic-ischemic brain damage. *Brain Res. Brain Res. Rev.* 29:137–168. doi:10.1016/S0165-0173(98)00053-8

Walton, M., A.M. Woodgate, A. Muravlev, R. Xu, M.J. During, and M. Dragunow. 1999b. CREB phosphorylation promotes nerve cell survival. *J. Neurochem.* 73:1836–1842.

Wan, H.I., A. DiAntonio, R.D. Fetter, K. Bergstrom, R. Strauss, and C.S. Goodman. 2000. Highwire regulates synaptic growth in *Drosophila. Neuron.* 26:313–329. doi:10.1016/S0896-6273(00)81166-6

Wang, M., Y. Wu, D.G. Culver, and J.D. Glass. 2001. The gene for slow Wallerian degeneration (Wld(s)) is also protective against vincristine neuropathy. *Neurobiol. Dis.* 8:155–161. doi:10.1006/nbdi.2000.0334

Wang, M.S., A.A. Davis, D.G. Culver, and J.D. Glass. 2002. WldS mice are resistant to paclitaxel (taxol) neuropathy. *Ann. Neurol.* 52:442–447. doi:10.1002/ana.10300

Weber, U., N. Paricio, and M. Mlodzik. 2000. Jun mediates Frizzled-induced R3/R4 cell fate distinction and planar polarity determination in the *Drosophila* eye. *Development.* 127:3619–3629.

Wharton, K.A., J.M. Cook, S. Torres-Schumann, K. de Castro, E. Borod, and D.A. Phillips. 1999. Genetic analysis of the bone morphogenetic protein-related gene, gbb, identifies multiple requirements during *Drosophila* development. *Genetics.* 152:629–640.

Wu, C., Y.P. Wairkar, C.A. Collins, and A. DiAntonio. 2005. Highwire function at the *Drosophila* neuromuscular junction: spatial, structural, and temporal requirements. *J. Neurosci.* 25:9557–9566. doi:10.1523/JNEUROSCI.2532-05.2005

Zhai, Q., J. Wang, A. Kim, Q. Liu, R. Watts, E. Hoopfer, T. Mitchison, L. Luo, and Z. He. 2003. Involvement of the ubiquitin-proteasome system in the early stages of wallerian degeneration. *Neuron.* 39:217–225. doi:10.1016/S0896-6273(03)00429-X

Zhai, R.G., F. Zhang, P.R. Hiesinger, Y. Cao, C.M. Haueter, and H.J. Bellen. 2008. NAD synthase NMNAT acts as a chaperone to protect against neurodegeneration. *Nature.* 452:887–891. doi:10.1038/nature06721